

大規模崩塌與大尺度邊坡模型沖 蝕崩塌試驗之震動訊號特性

馮正一

國立中興大學水土保持學系
教授兼系主任

tonyfeng@nchu.edu.tw

大綱

- 大規模崩塌震動訊號
- 崩塌震動訊號特性
- 大尺度邊坡模型沖蝕崩塌試驗初步成果
- 未來研究構思

大規模崩塌震動訊號

Seismic recordings of landslides caused by Typhoon Talas (2011), Japan By Yamada, et al. (2012 in GRL)

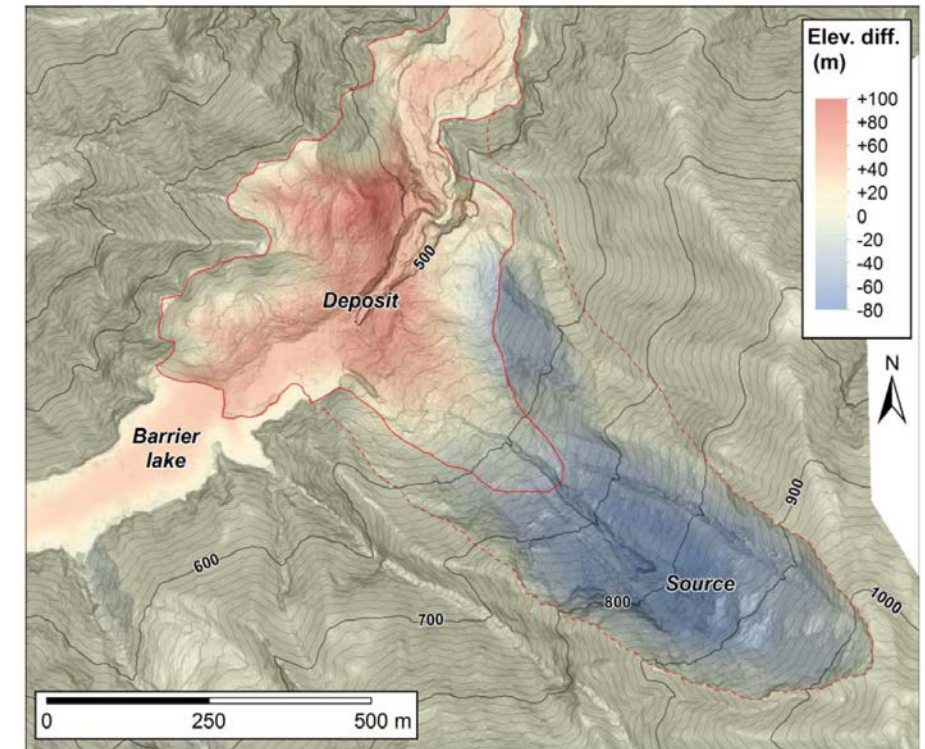
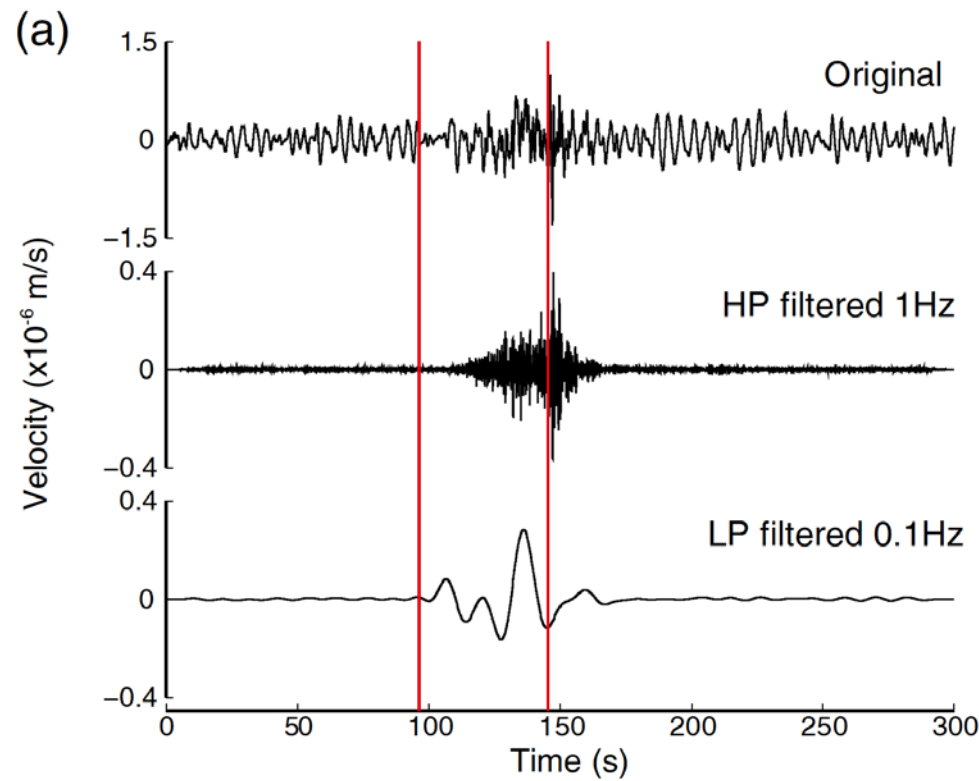


Fig. 1 (a) Broadband seismic records of Akatani landslide at NOKF station. The vertical lines show the onset and approximate time of impact on the far valley wall. Original record, high-pass filtered record at 1Hz, low-pass filtered record at 0.1Hz from the top.

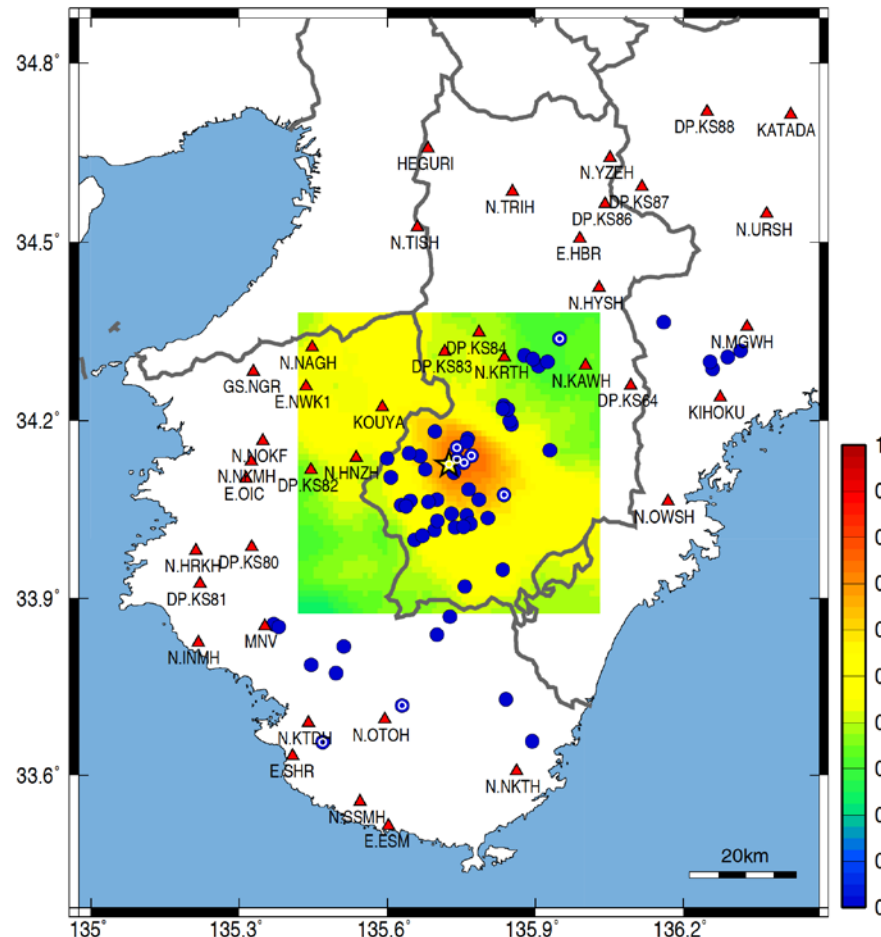


Fig. 2 Distribution of the seismic stations (triangles) and landslides (circles). Landslides identified by seismic records are marked with white circles. The shaded colors show the probability of the location of Akatani landslide, obtained from the back-projection analysis. The star shows the surface location of the Akatani landslide.

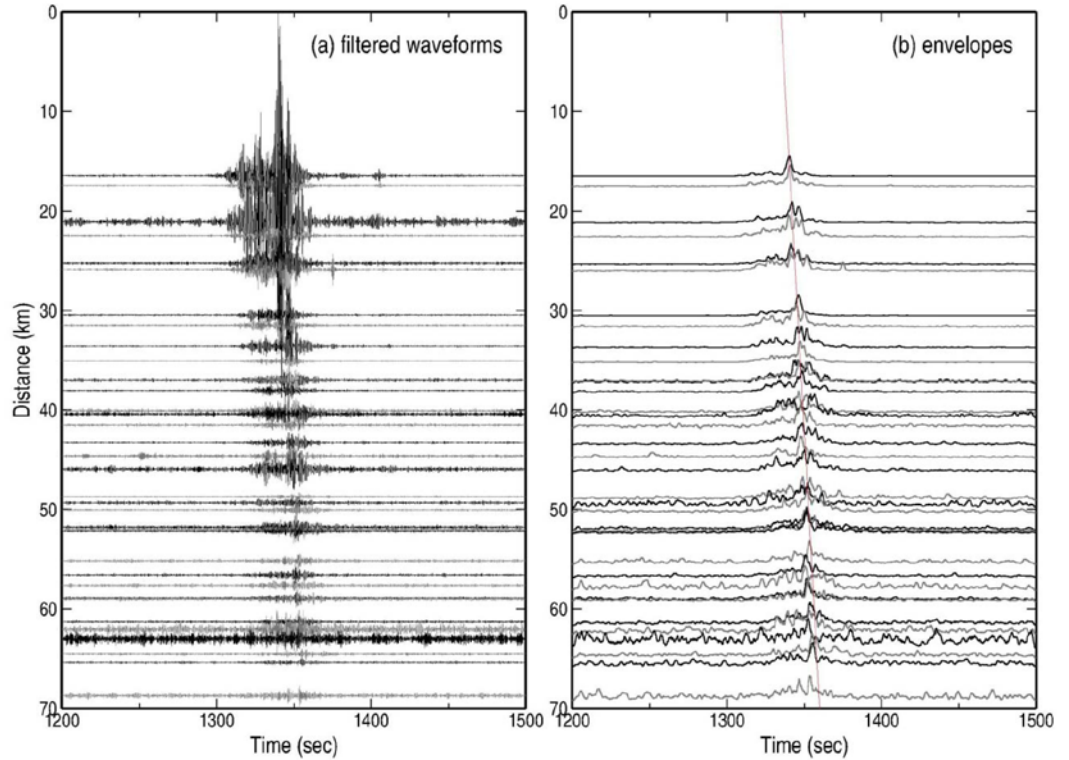


Fig. 3 Seismic records of the Akatani landslide. (a) 1-4Hz band-pass filtered records, (b) processed envelopes for back-projection analysis. Adjacent seismograms are shown alternatingly in black and gray for clarity. The red line shows the predicted arrival time for the location obtained from the back-projection analysis.

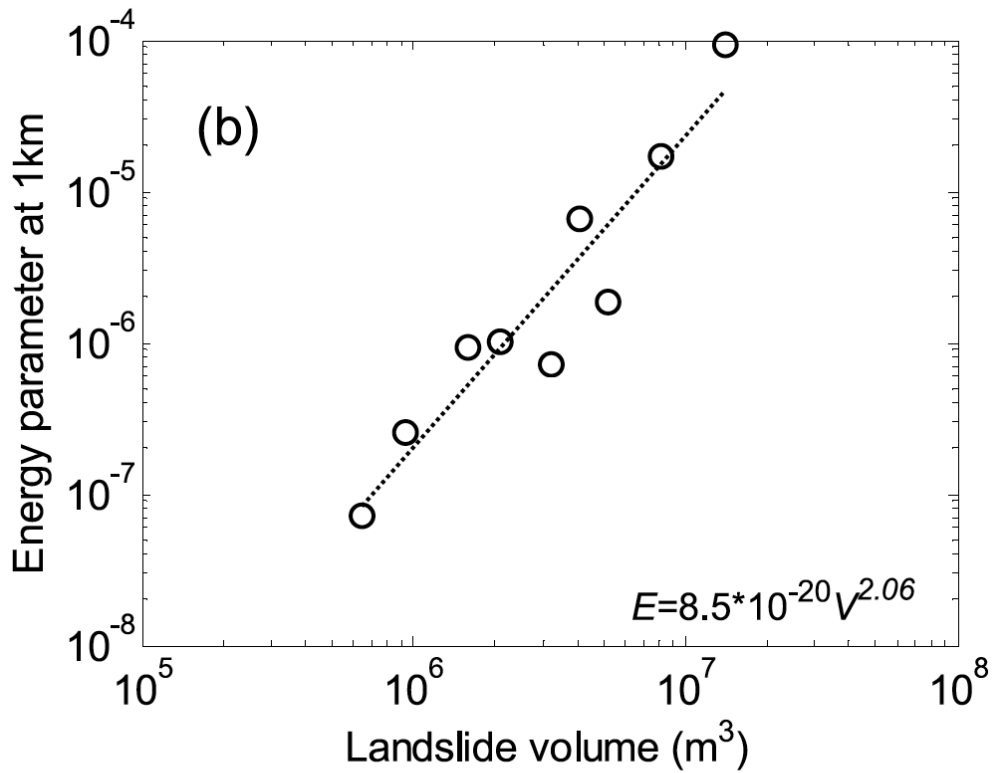
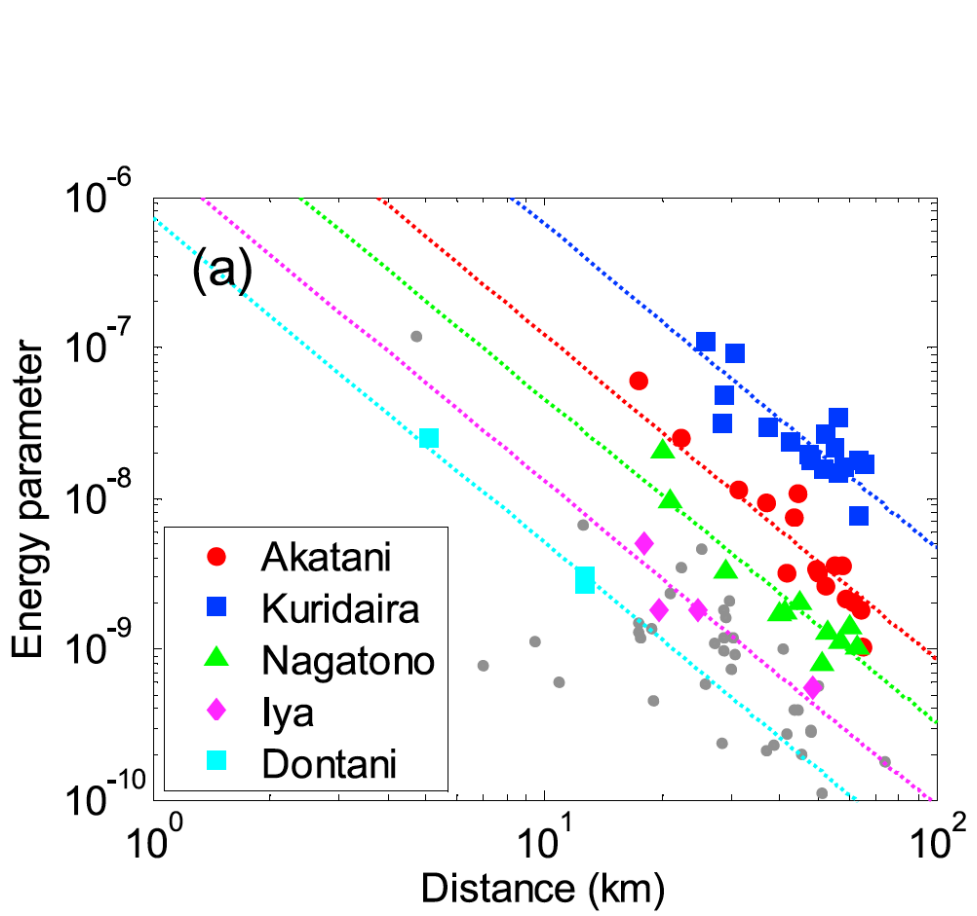
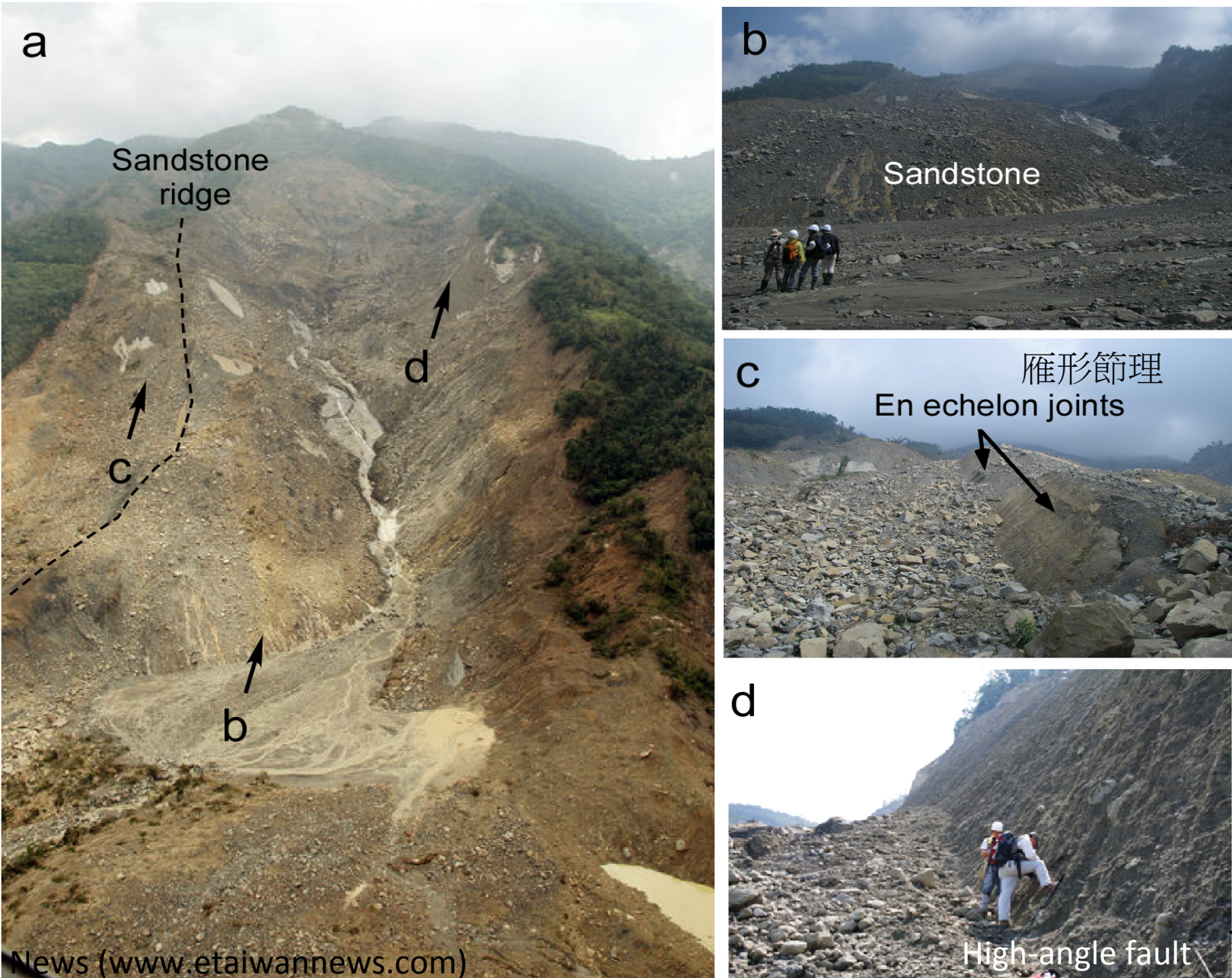
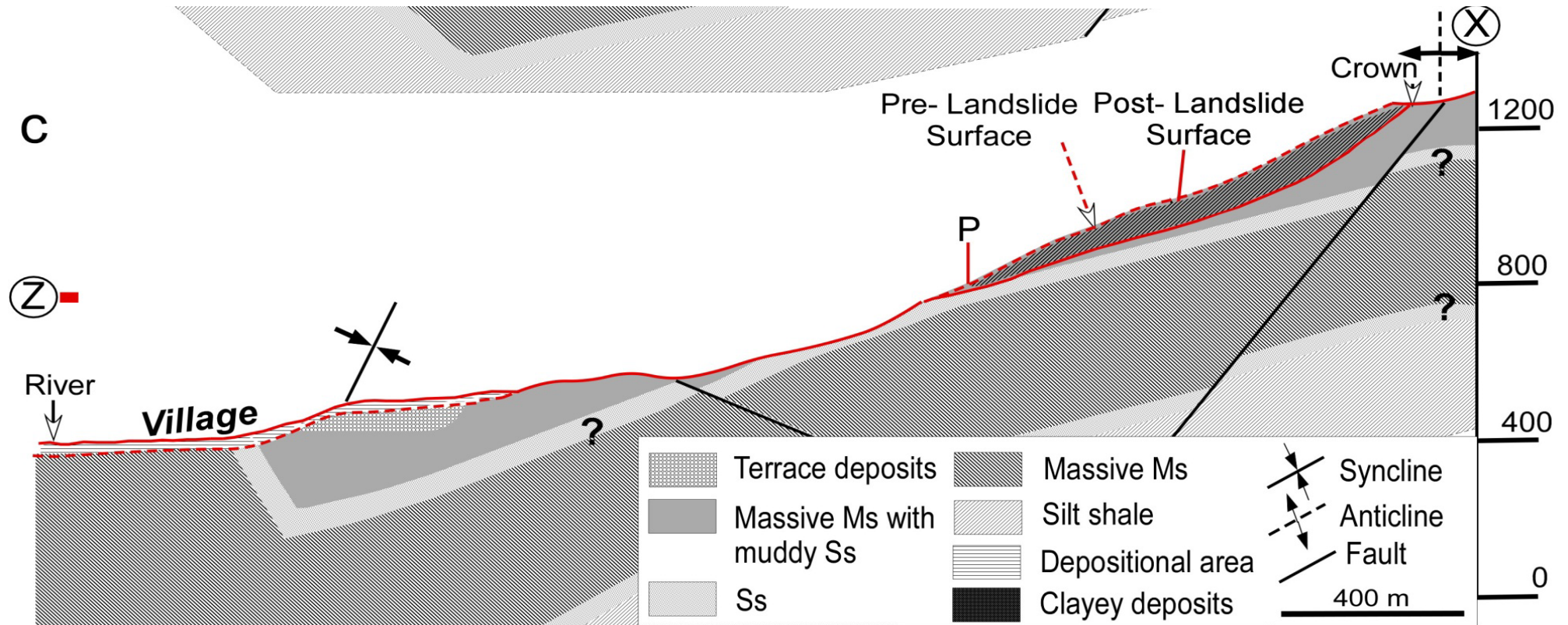


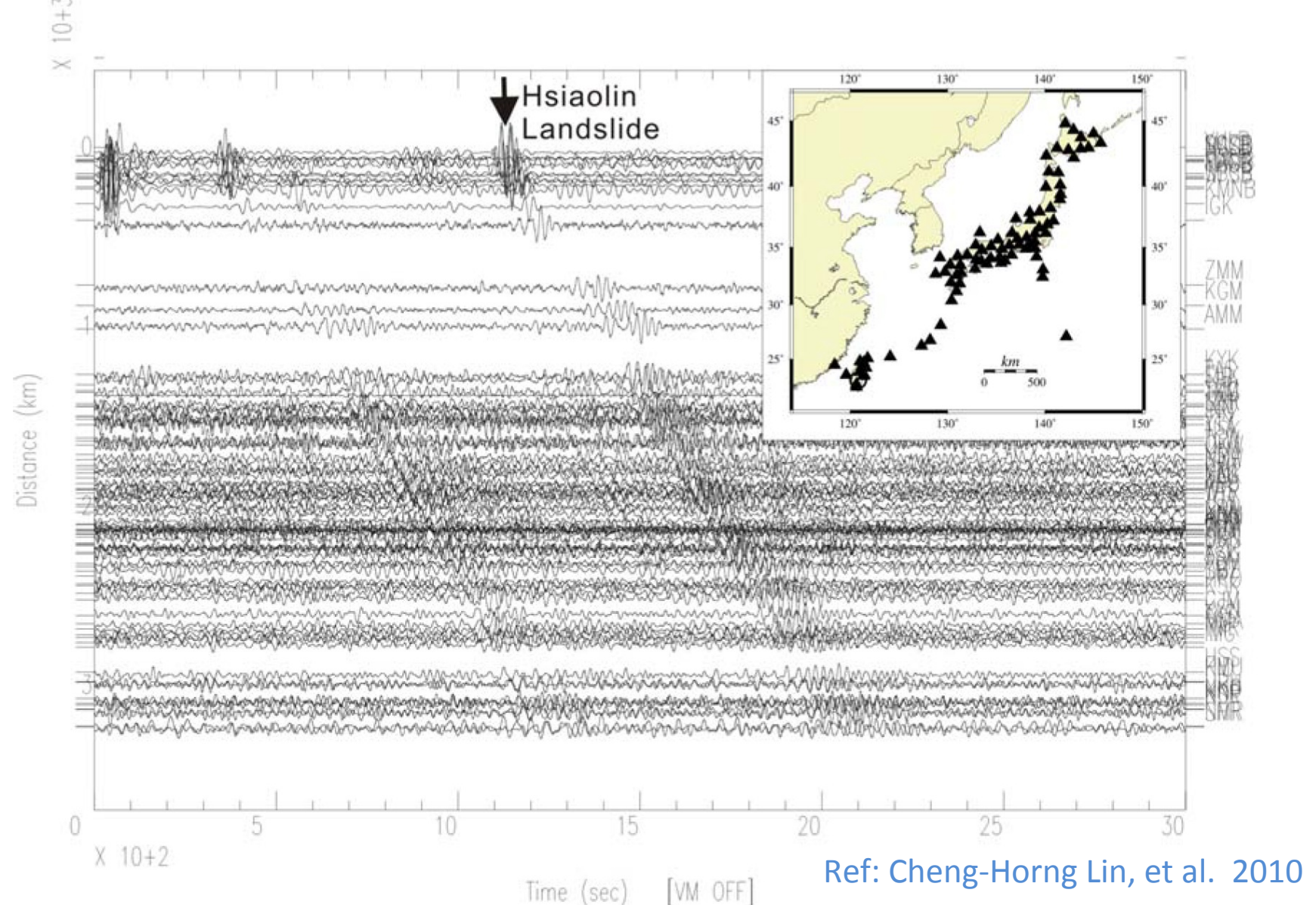
Figure 4. (a) Energy parameter of different landslides as a function of source-station distance. The lines show regression functions for each event. (b) Relationship between volume of the landslide and the energy parameter for a distance 1 km from the source. The line and equation in the figure show the results of a linear regression.

Ching-Ying Tsou, Zheng-Yi Feng, Masahiro Chigira (2011)





1 Supplementary material:

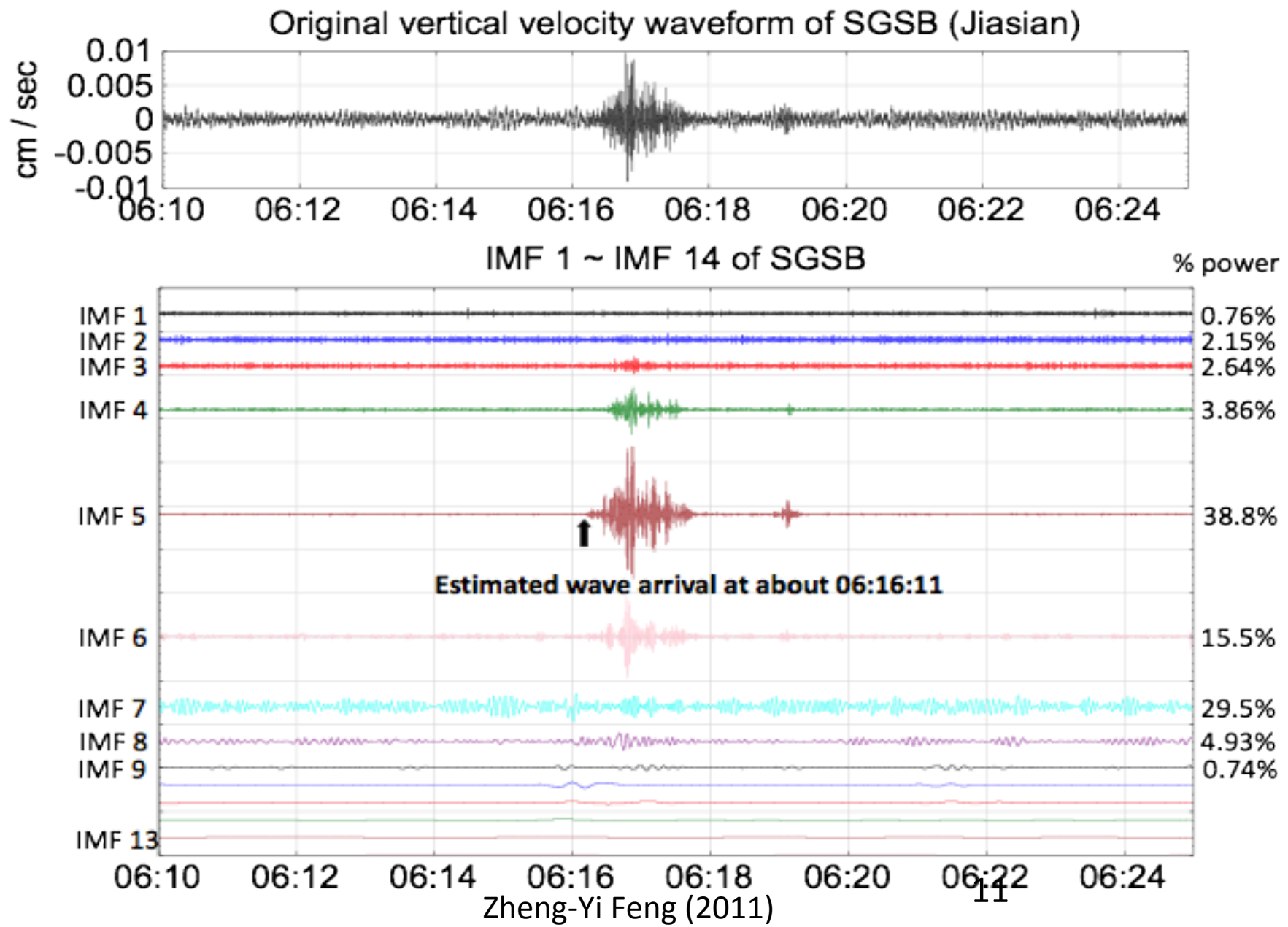


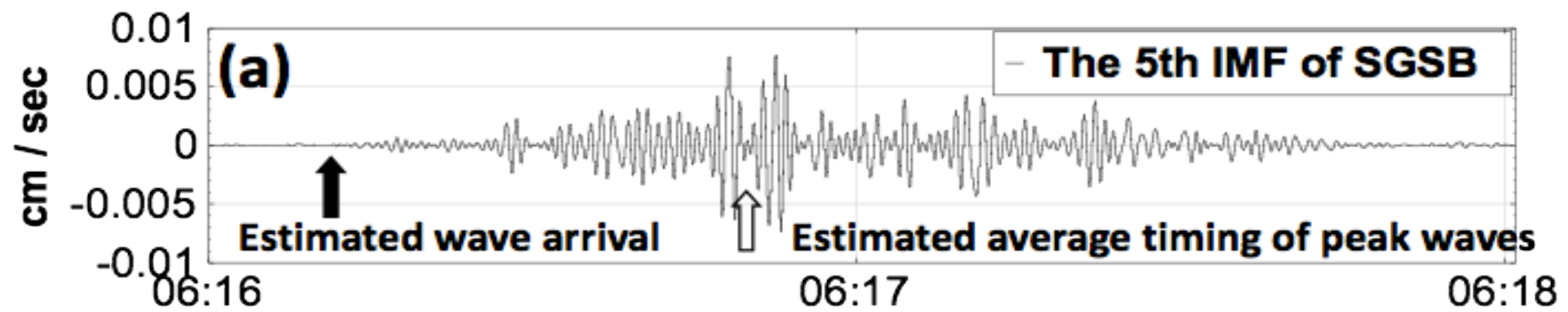
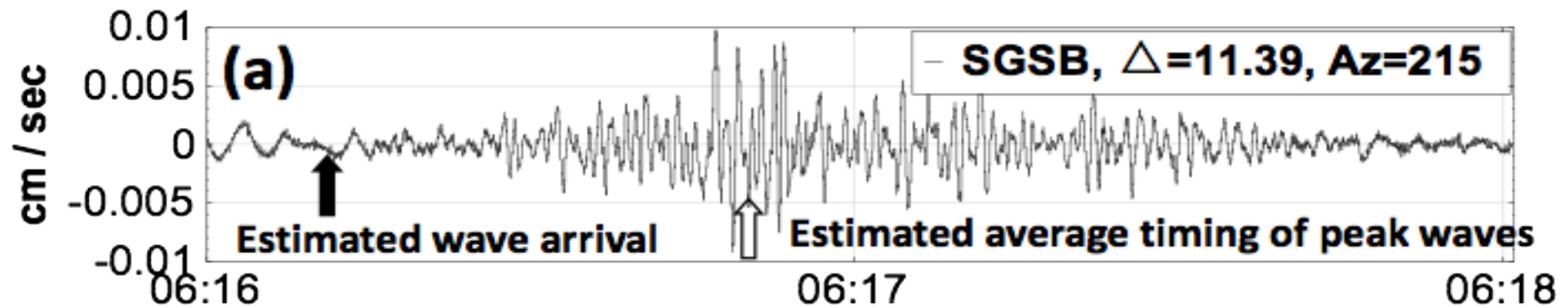
2
3 Fig. S1 Long period seismic signals generated by the Hsiaolin landslide and
4 recorded at all broadband seismic stations in Taiwan and Japan.



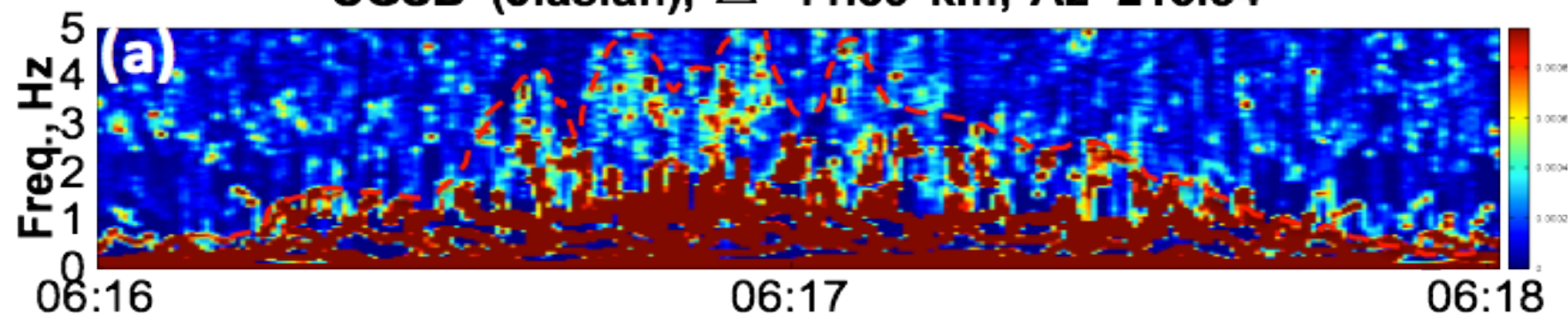
Captured from internet.

Xiaolin LS Seismic signal at SGSB station





SGSB (Jiasian), $\Delta=11.39$ km, Az=215.54



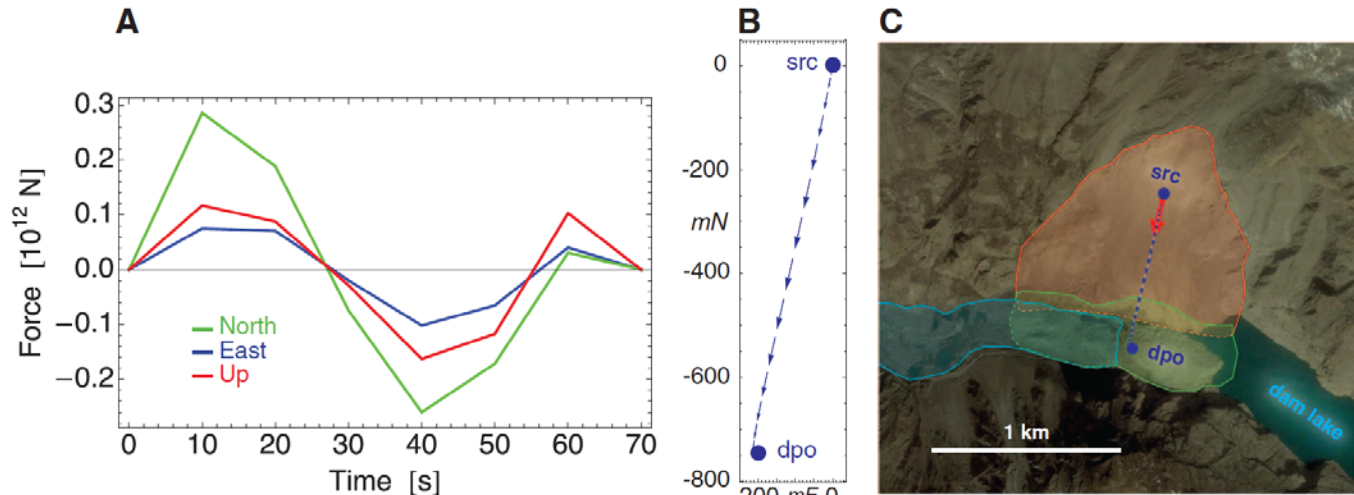
Key points of the LS vibration

- The main frequency contents of the seismic waves caused by the Xiaolin landslide were in the range of **0.5 to 1.5 Hz**.

Published in *Z. Feng, Nat. Hazard Earth Sys. 11, 1559 (2011)* and cited by *Petley (2013) "Characterizing Giant Landslides", Science*, DOI: 10.1126/science.1236165.

Ekstrom and Stark (2013) “Simple Scaling of Catastrophic Landslide Dynamics”, Science 339, 1416

Fig. 1. Landslide force history and trajectory for the Hunza-Attabad landslide. (A) Inversion of the landslide force history $\mathbf{F}(t)$ (LFH) of this event, pinning the time of main failure at 08:37 UT (table S1). (B) The planform trajectory of landslide motion deduced by doubly integrating the LFH and scaling by the runout distance mapped in (C). (C) Satellite-image mapping of the landslide scar and runout. The estimated centers of the source (“src”) and deposits (“dpo”) are indicated; their spatial separation was used to estimate D_h , determine the effective mass, and scale the displacement trajectory $\mathbf{D}(t)$.



22 MARCH 2013 VOL 339 SCIENCE www.sciencemag.org

No.	Name	Date UT	Time UT	Location °N	Location °E	M_{SW}	F_{max} 10^{12} N	p_{max} 10^{12} kg m s ⁻¹	ΔE 10^{15} J	Δt s	m 10^{12} kg	D_z m	D_h m	$ v _{max}$ m s ⁻¹
1	Mt St Helens	1980/05/18	15:32	46.21	-122.19	5.6	4.470	225.00	38.000	220	2.500	1549	7753	90.0
2	Valpola	1987/07/28	05:24	46.38	10.34	5.4	0.543	7.03	0.497	70	0.108	469	1441	65.1
3	Kaiapit	1988/09/06	00:42	-6.12	146.30	5.3	1.470	49.10	4.420	135	0.729	618	4512	67.3
4	Randa #1	1991/04/18	04:41	46.11	7.77	4.9	0.031	0.53	0.094	60	0.044	217	277	12.1
5	Randa #2	1991/05/09	18:52	46.11	7.77	4.8	0.053	0.74	0.102	70	0.034	307	646	21.8
6	Conchut	1999/11/07	18:03	-6.41	-78.47	5.0	0.134	2.52	0.072	90	0.090	81	1219	28.1
7	Yìgōng	2000/04/09	12:00	30.24	94.99	5.5	1.020	29.00	4.120	165	0.440	955	5229	65.9
8	Mt Garmo	2001/09/02	16:57	38.79	72.08	5.4	0.749	16.20	1.520	80	0.284	547	2190	57.3
9	Mt Steller	2005/09/14	19:59	60.52	-143.09	5.2	0.267	6.42	1.370	110	0.081	1725	3275	79.3
10	Mt Steele	2007/07/25	00:57	61.11	-140.30	5.2	0.283	7.60	0.523	110	0.108	494	3354	70.4
11	Hsiäolín	2009/08/08	22:16	23.17	120.65	5.0	0.110	2.72	0.366	110	0.060	624	2253	45.5
12	Táoyuán	2009/08/09	02:52	23.22	120.76	4.9	0.142	2.85	0.224	90	0.252	91	393	11.3
13	Fāngtúnshān #2	2009/08/09	09:32	22.56	120.81	5.2	0.384	6.36	0.466	100	0.134	354	1933	47.4
14	Fāngtúnshān #1	2009/08/09	09:32	22.56	120.81	--	0.058	0.72	0.043	45	0.013	337	1116	55.4
15	Fùxíng	2009/08/10	11:06	23.23	120.76	4.9	0.084	1.24	0.123	130	0.052	240	959	23.9

Morakot
2009

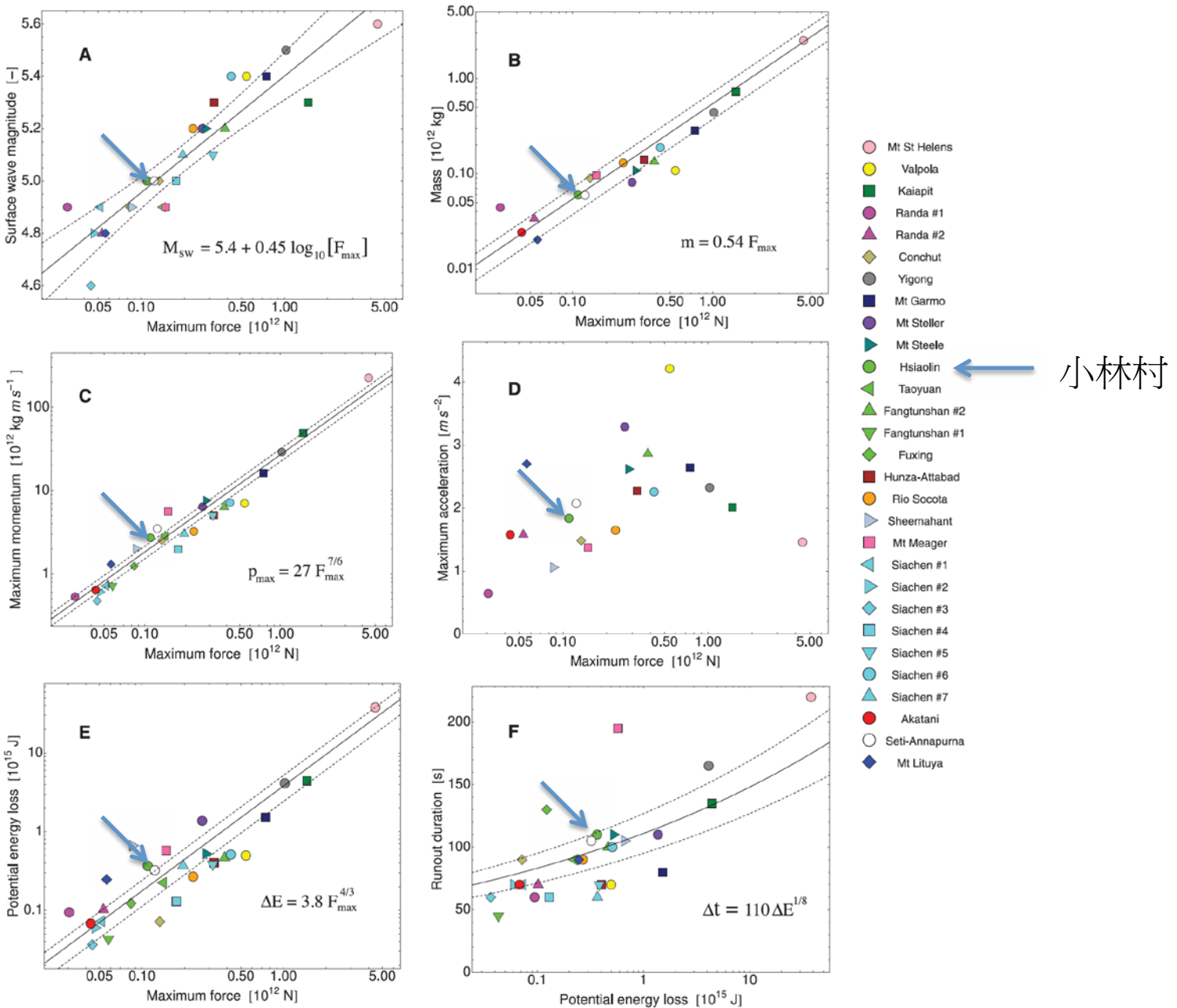


Fig. 2. Maximum force F_{\max} versus (A) long-period surface-wave magnitude M_{SW} , (B) mass m , (C) maximum momentum p_{\max} , (D) maximum acceleration a_{\max} , and (E) potential energy loss ΔE . Runout duration Δt versus potential energy loss ΔE is shown in (F). In (A) to (C), (E), and (F), the solid lines show model fits and the dashed lines indicate model mean confidence intervals at the 99% level.

崩塌震動訊號特性

- 以顆粒流程式(PFC)與連體程式(FLAC)耦合方法，以小林村崩塌為案例，建立山崩滑動過程之數值模型，探討山崩產生的震動特性與進行參數分析。

Why PFC?

Landslide videos

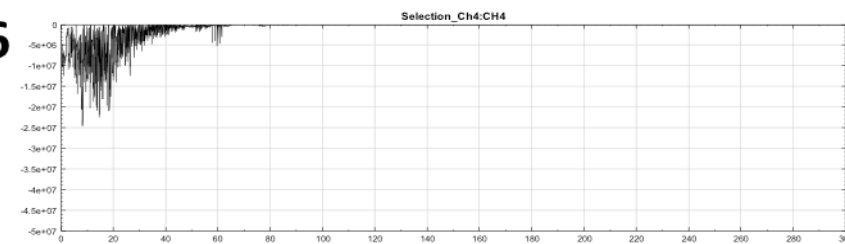
- [Video Clip 1](#)
- [Video Clip 2](#)
- [Video Clip 3](#)

PFC simulation Only

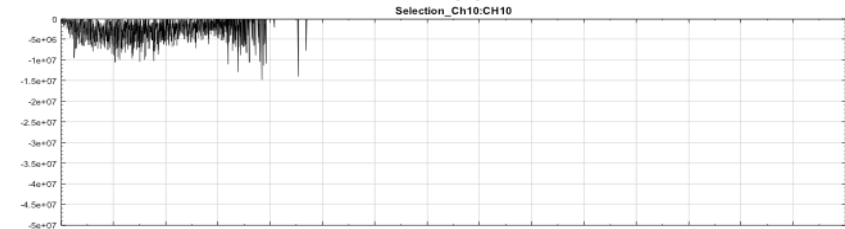
Y-force vs time & time-frequency
analysis

Fig. 6

A



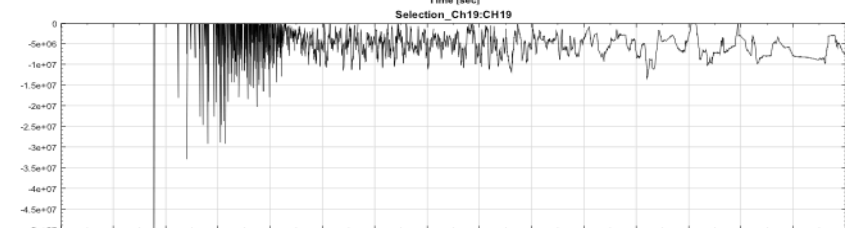
B



C



D



E

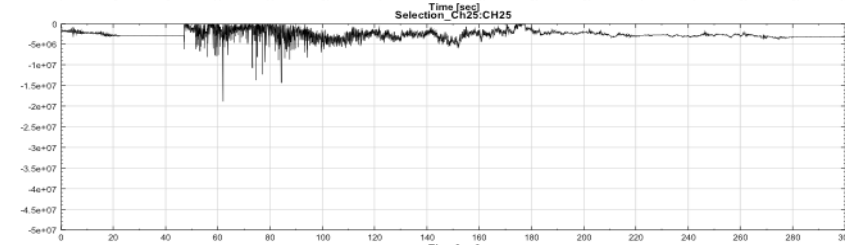
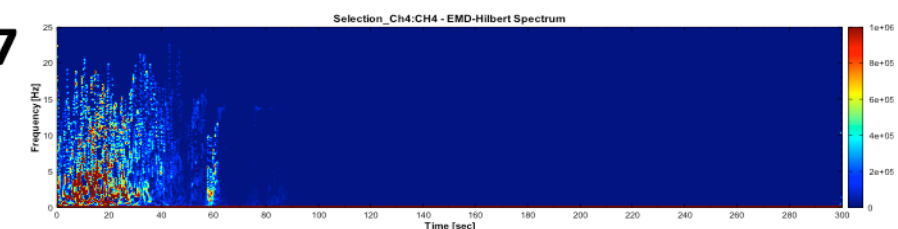
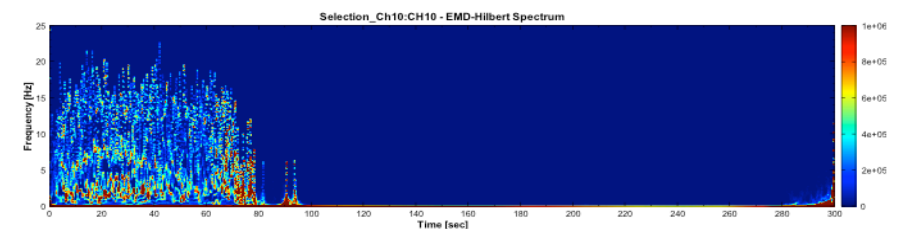


Fig. 7

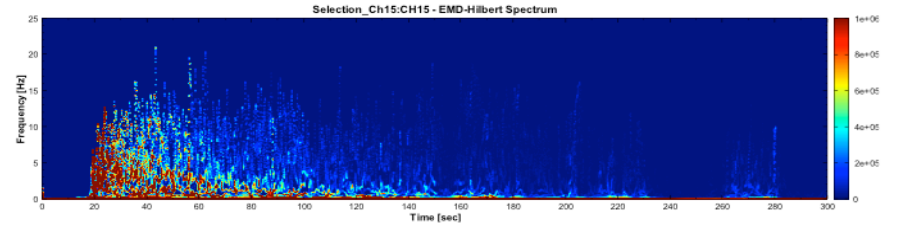
A



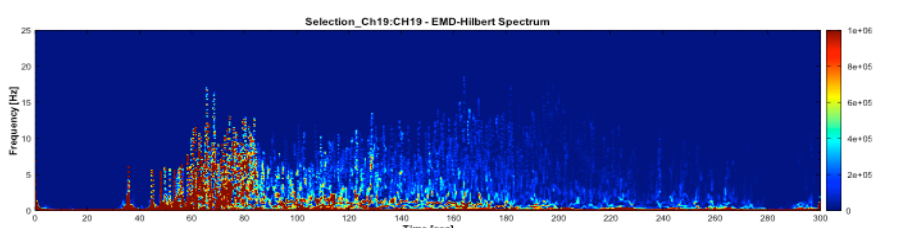
B



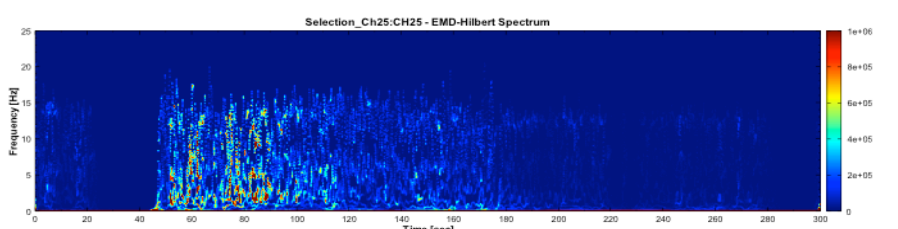
C



D



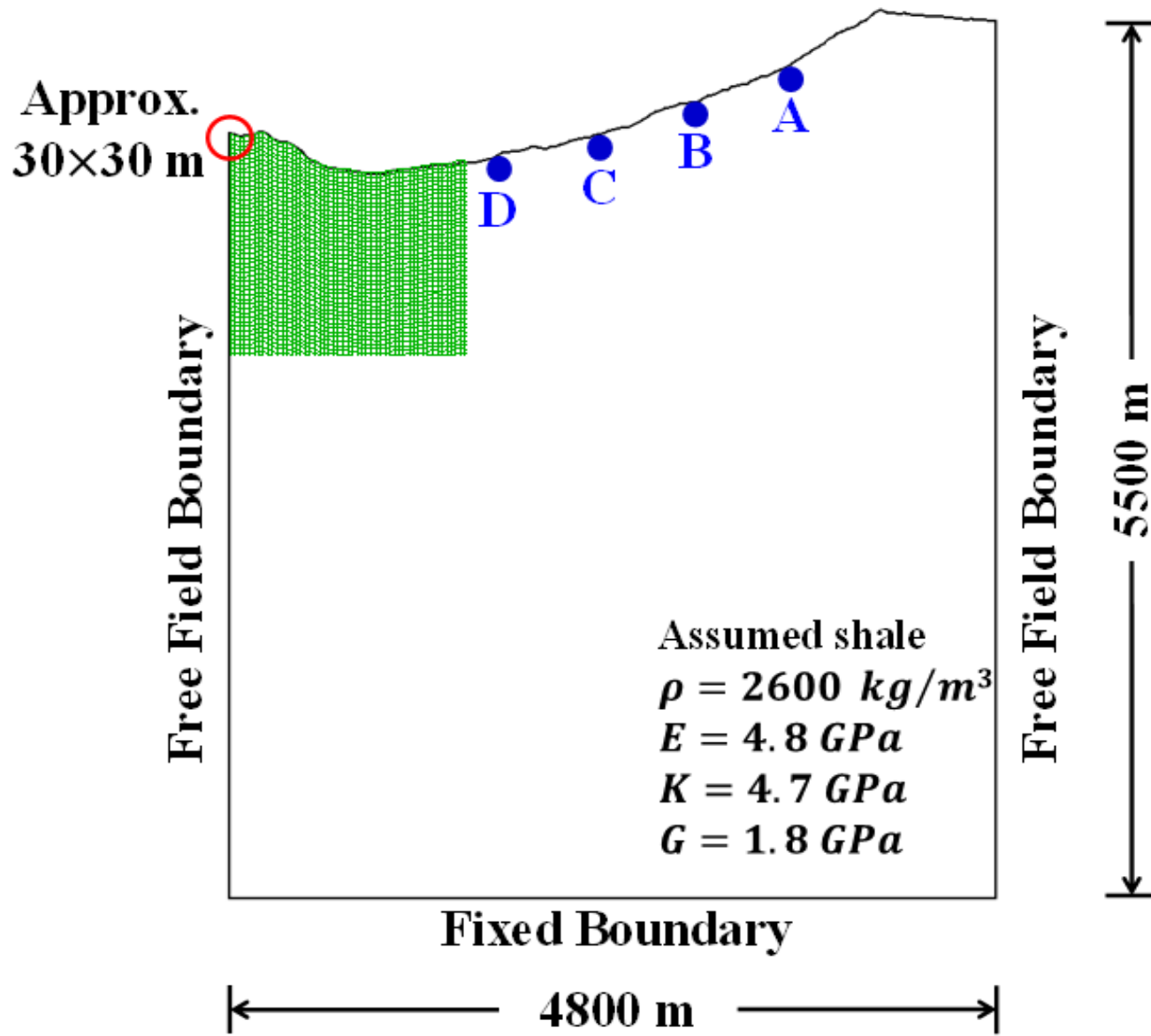
E



Why FLAC?

PFC and FLAC coupling for Seismic signals of landslides

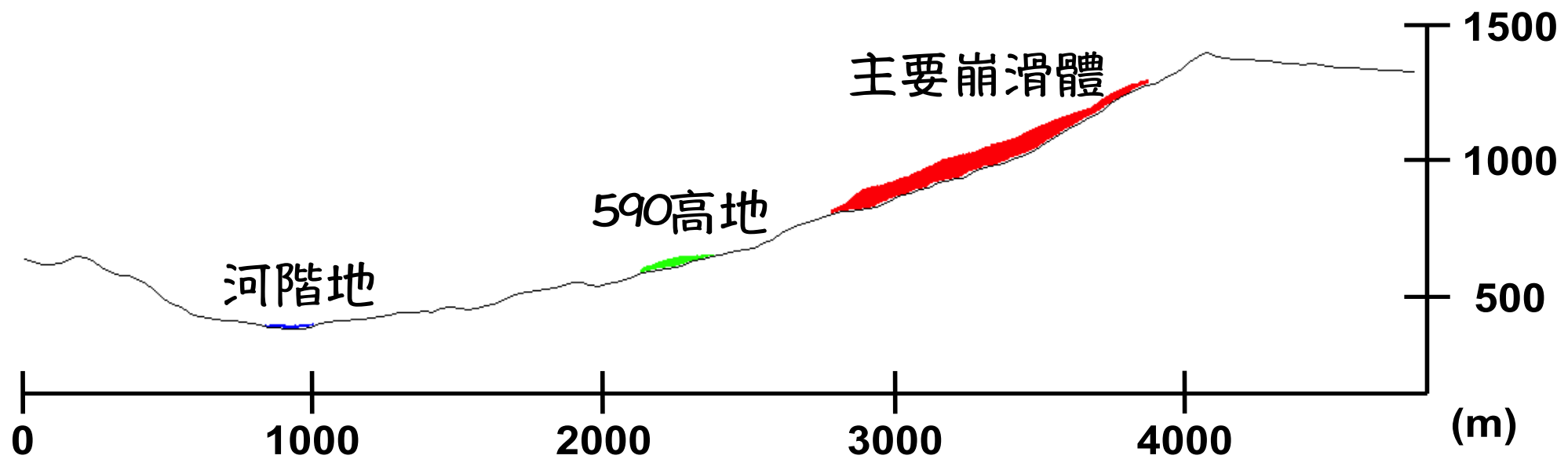
- 本研究以離散元素方法(PFC)模擬山崩產生的岩塊散開、滑動與流動過程
- 當岩塊撞擊有限差分數值模型(FLAC)構成的連體網格時，兩程式在同一「時階(timestep)內」可以耦合(coupling)會相互交換力量「參數」
- 而FLAC所記錄之歷時(history)更能完整呈現山崩之震動訊號。



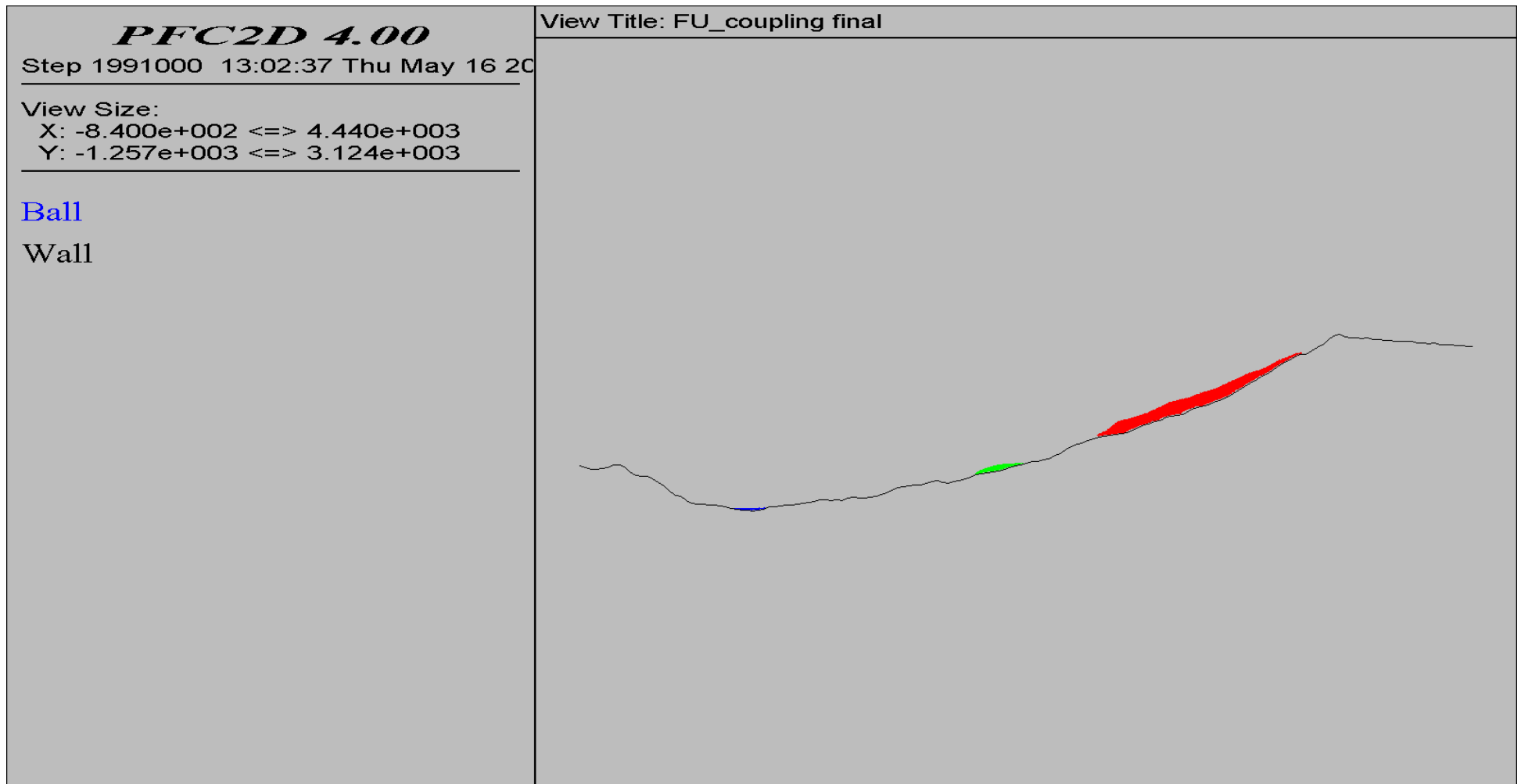
The FLAC numerical model

Baseline case – 崩滑體

- 顆粒摩擦係數 0.08
- Wall friction 0.5
- 顆粒半徑範圍分別設定為0.5~2 m
- FLAC mesh size about 30 m x 30 m
- 正向鍵結強度設定為16 MPa，切向鍵結強度設為正向鍵結強度的一半
- 正向黏滯阻尼係數0.4及切向黏滯阻尼係數0.2
- ...



- The simulation of PFC + FLAC



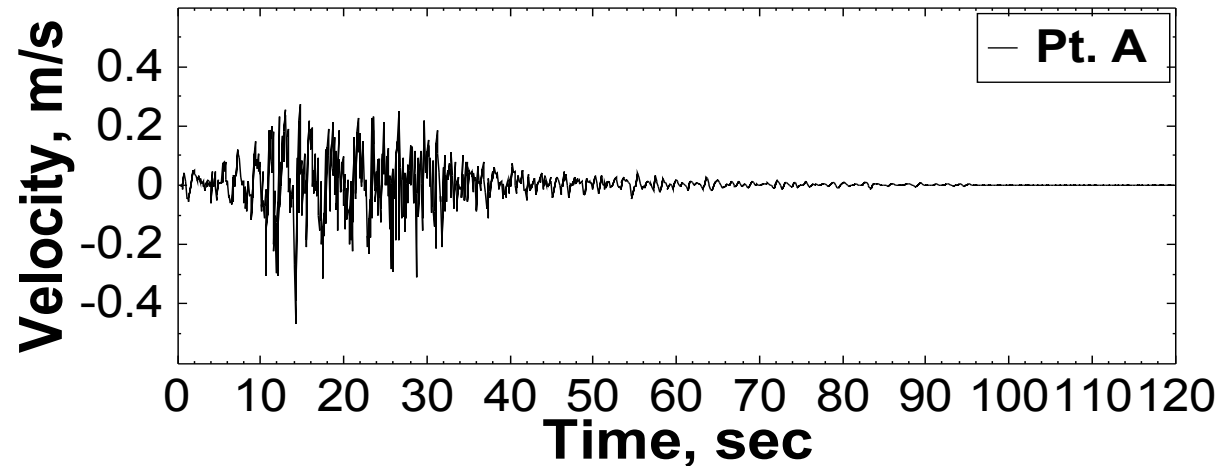


圖9 基線案例之垂直向速度(監測點A)

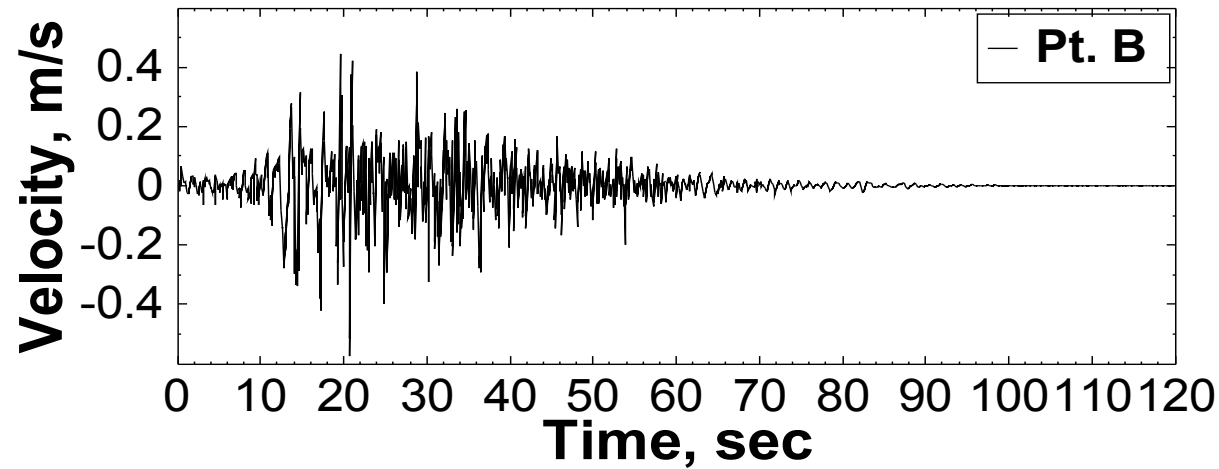


圖10 基線案例之垂直向速度(監測點B)

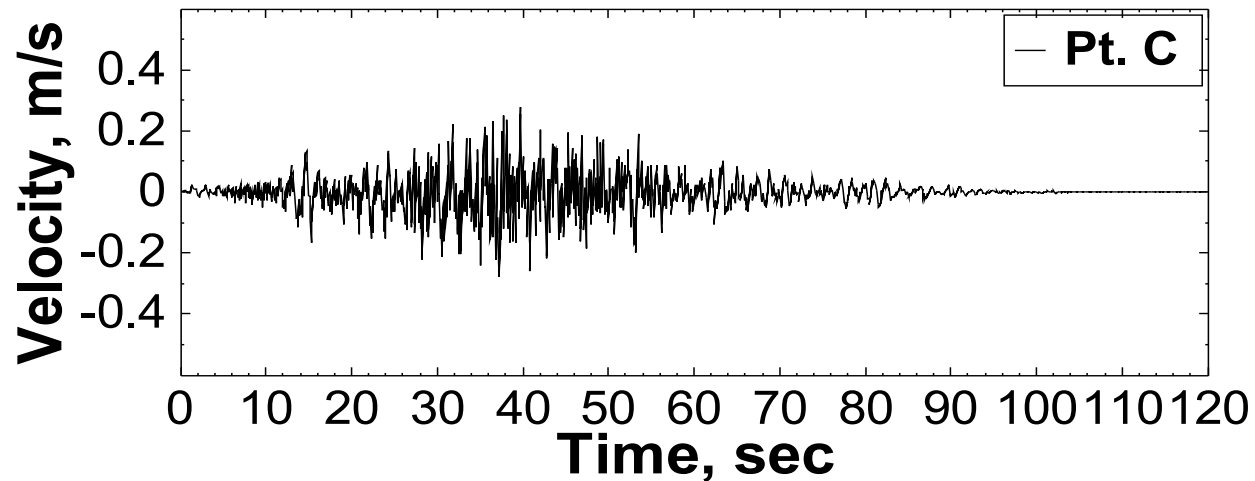


圖11 基線案例之垂直向速度(監測點C)

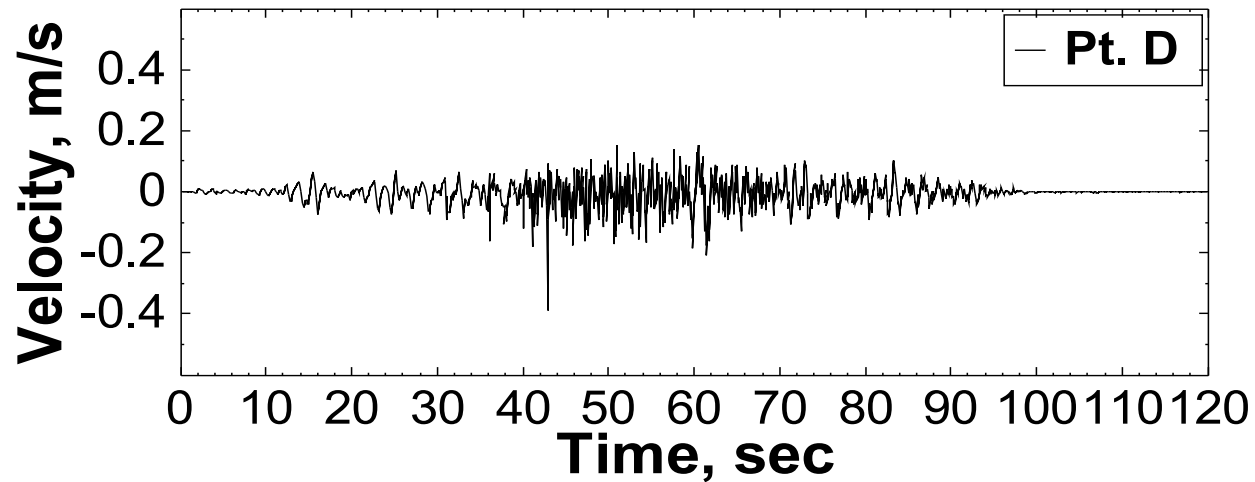


圖12 基線案例之垂直向速度(監測點D)

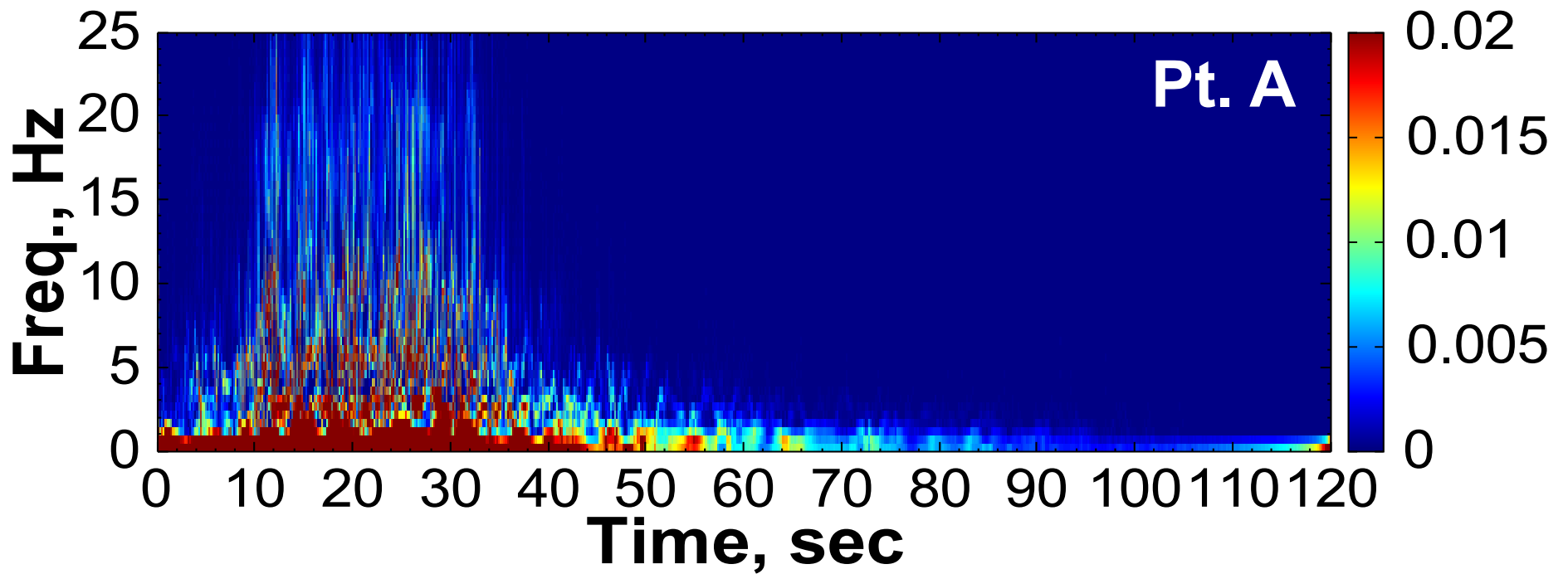


圖15 基線案例之時頻圖 (監測點A)

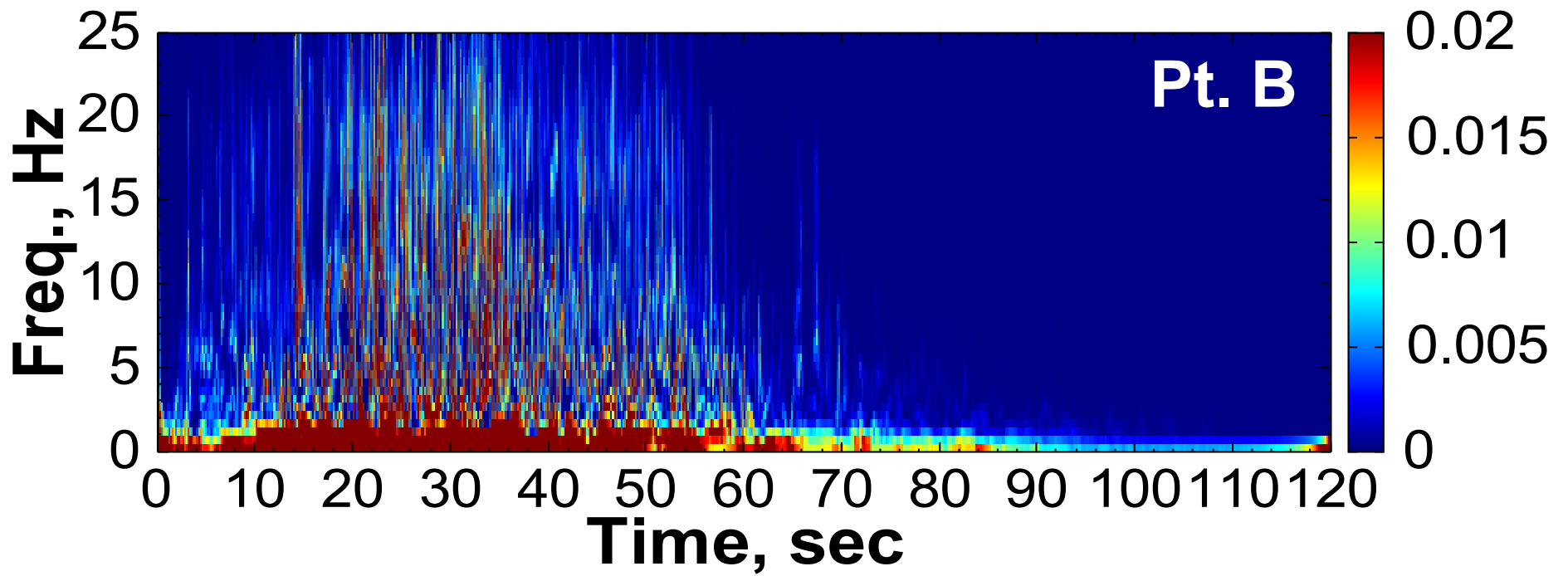


圖16 基線案例之時頻圖 (監測點B)

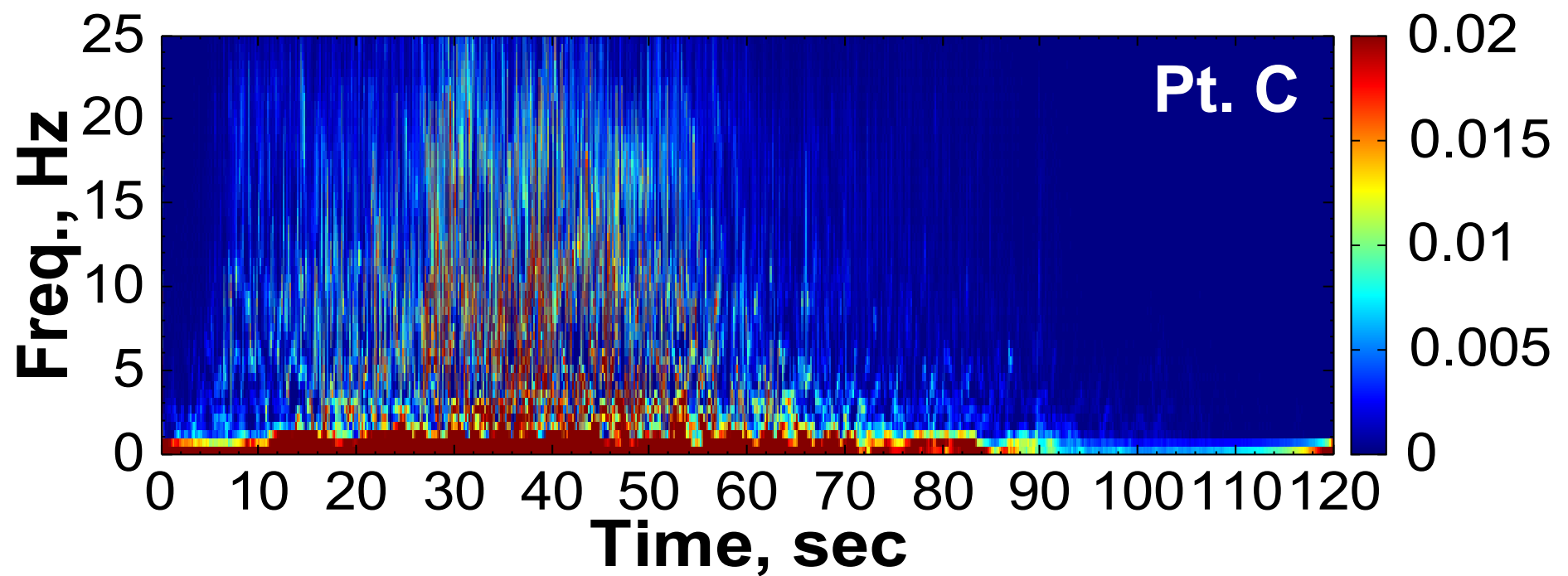


圖17 基線案例之時頻圖 (監測點C)

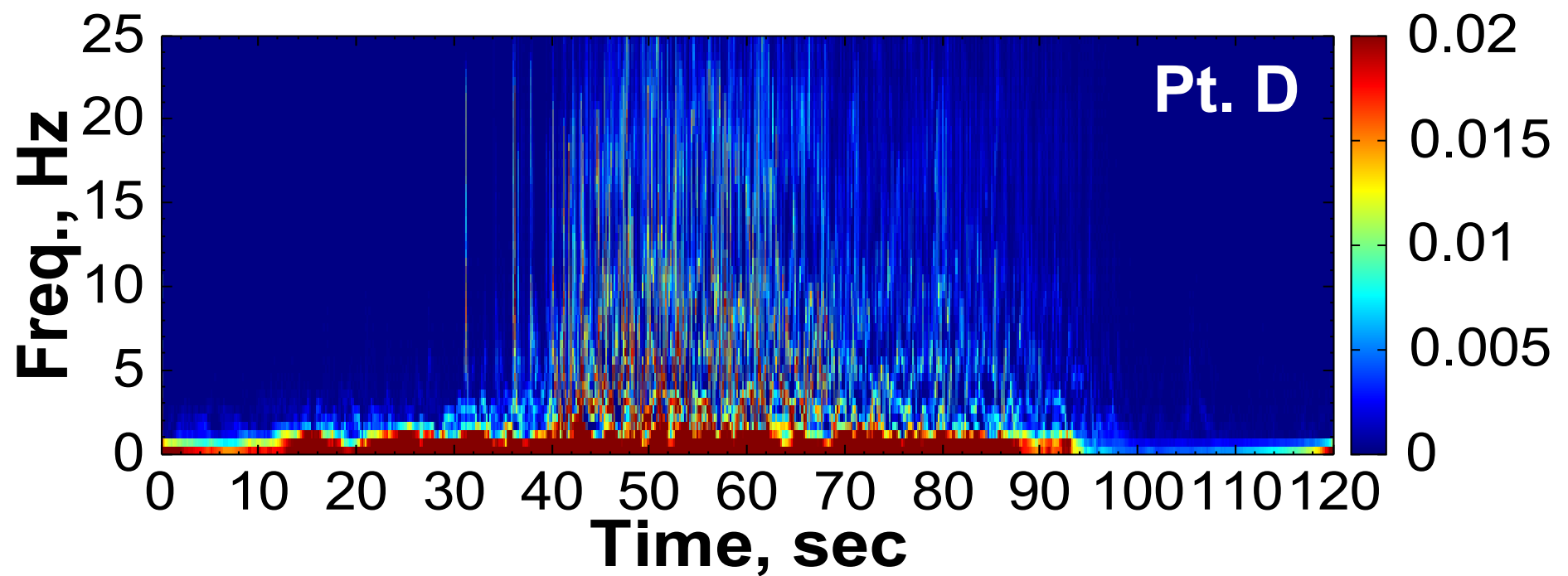
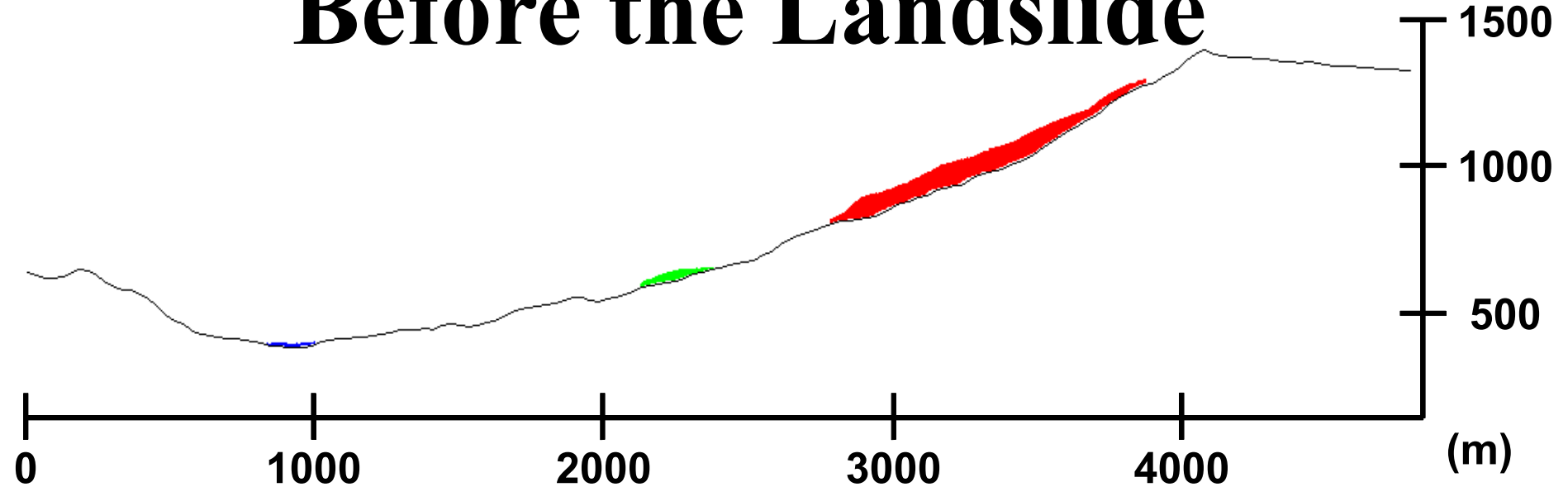
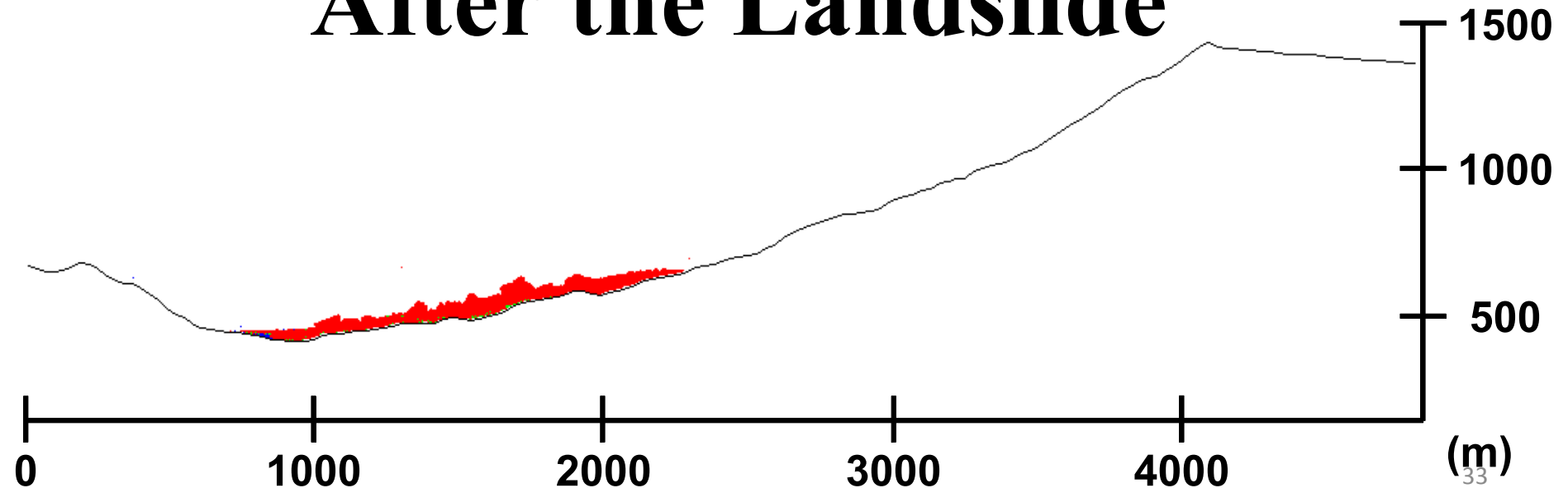


圖18 基線案例之時頻圖 (監測點D)

Before the Landslide



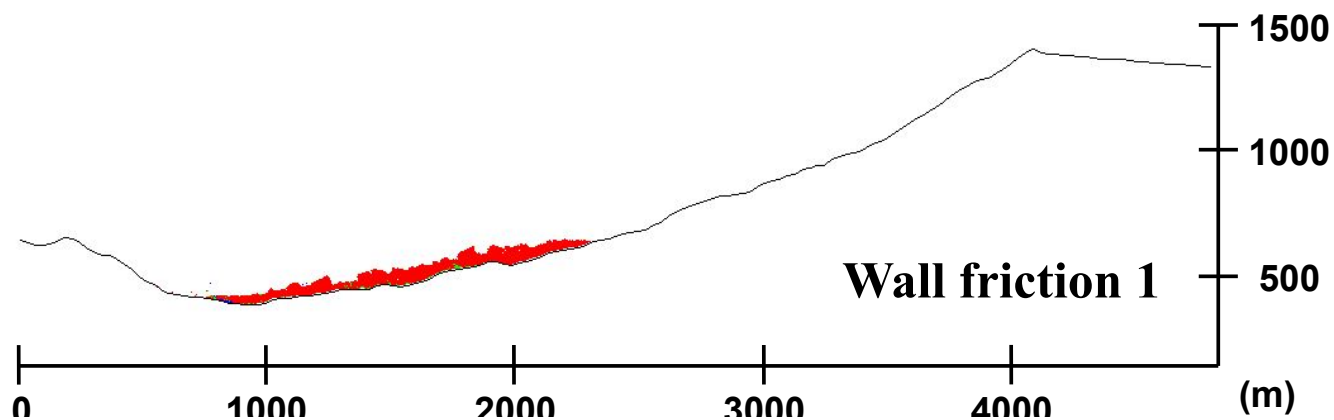
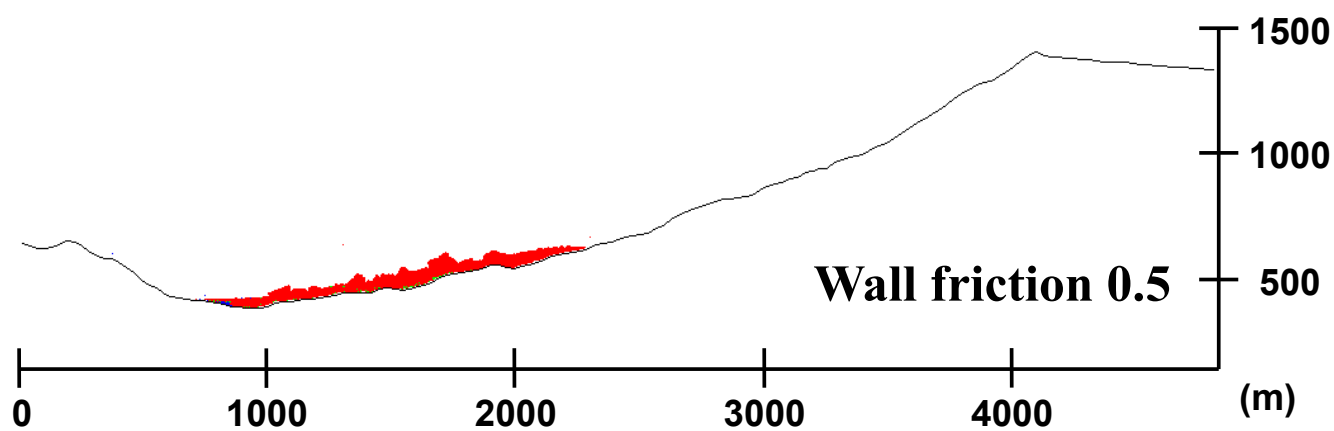
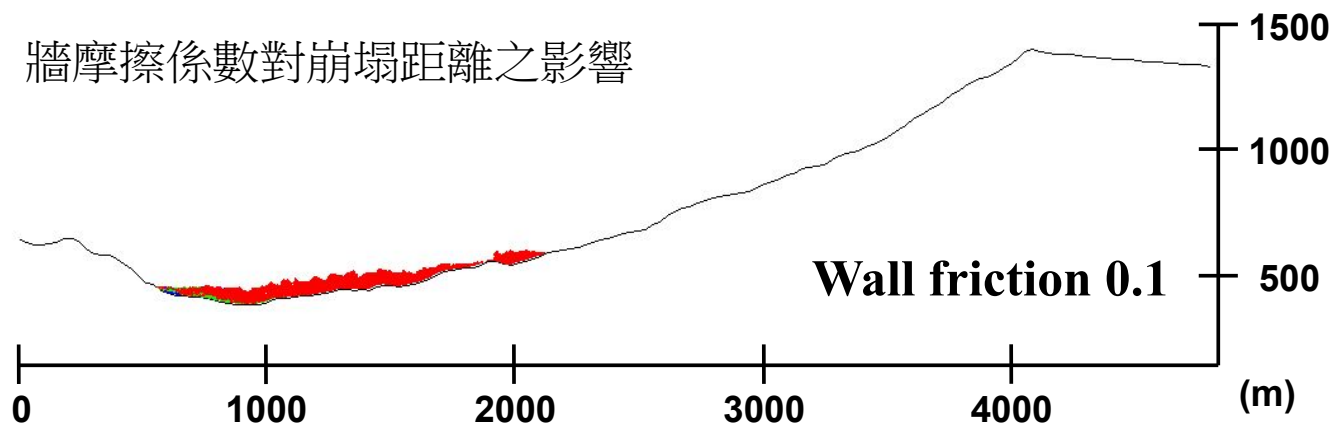
After the Landslide



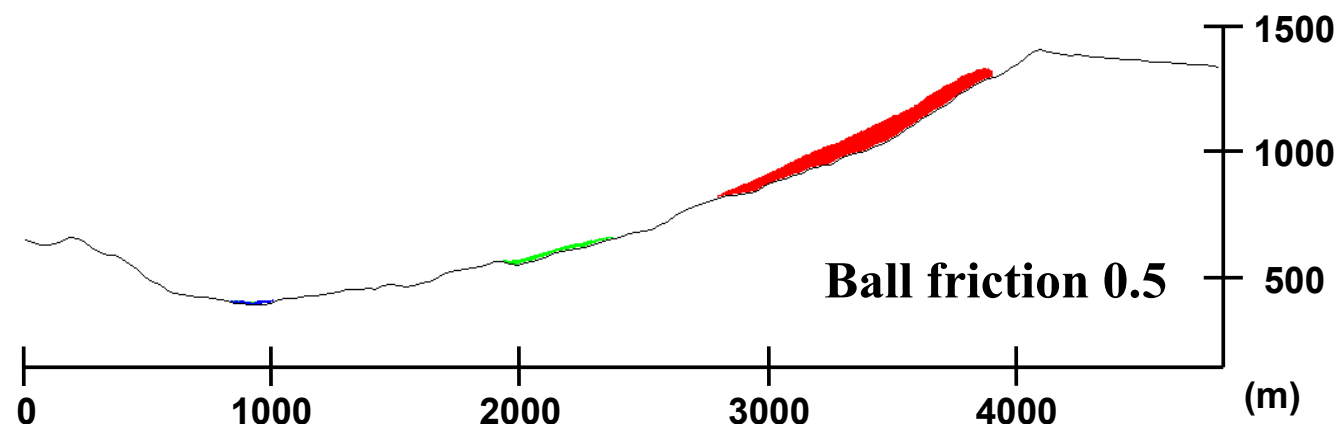
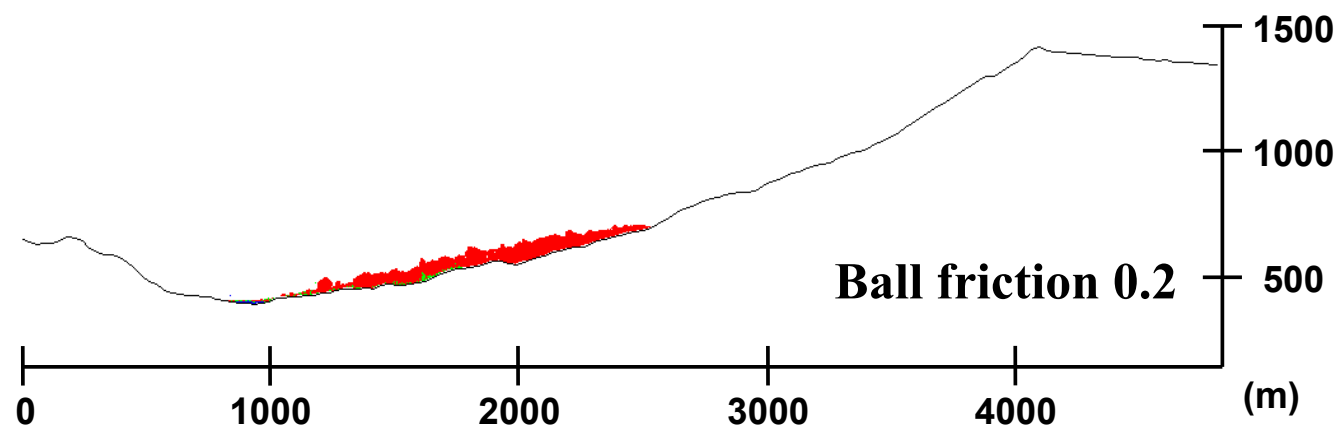
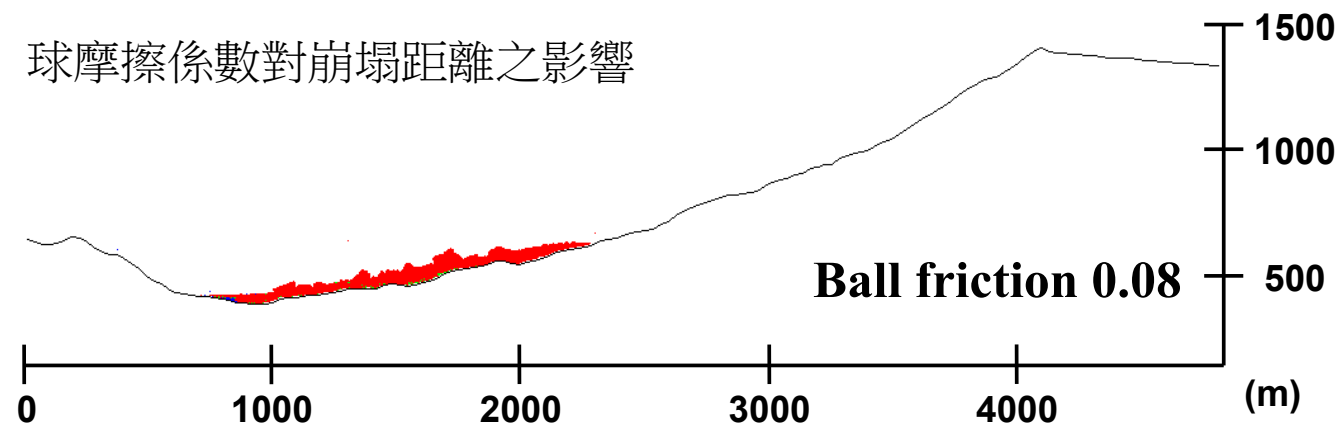
Parametrical study

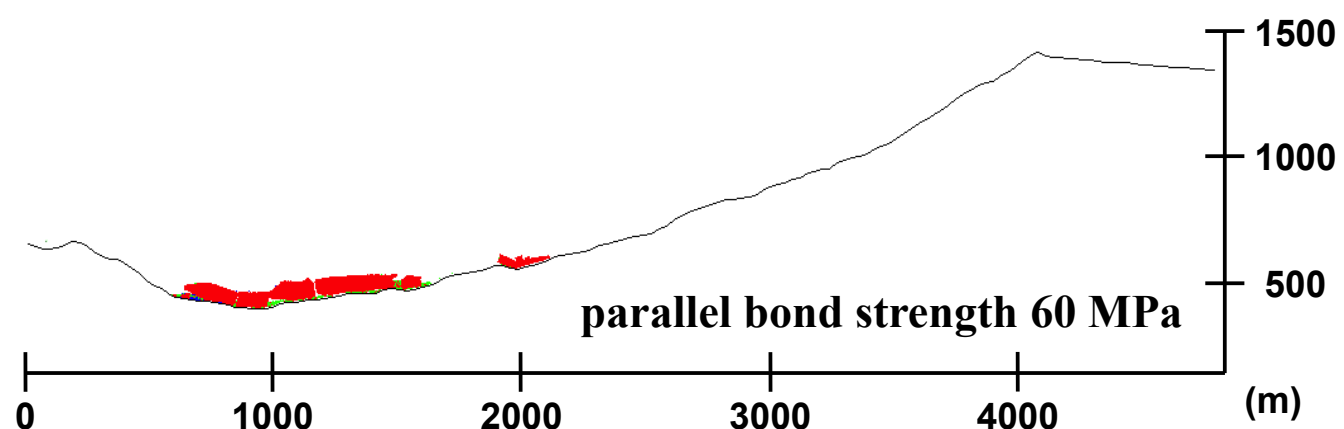
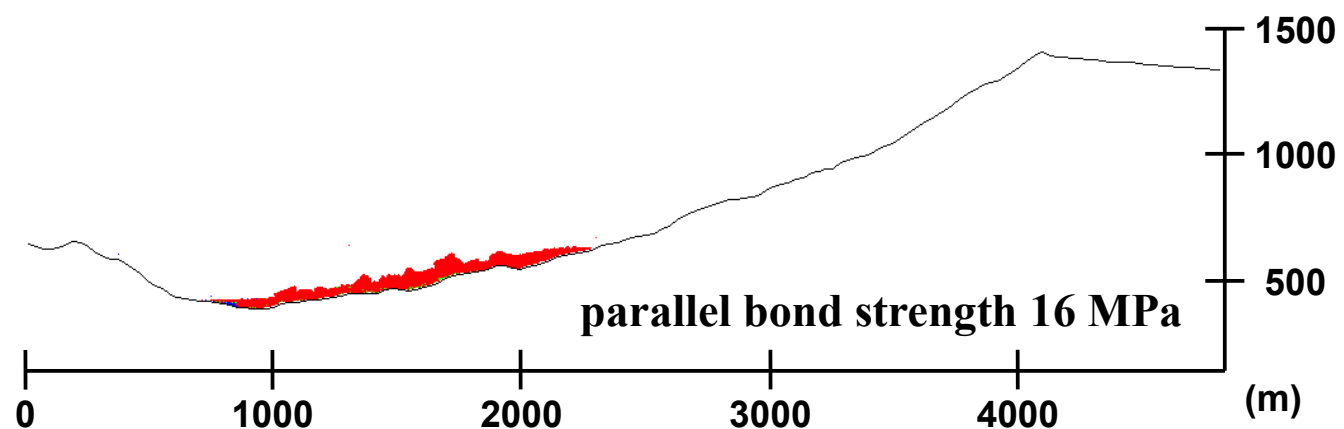
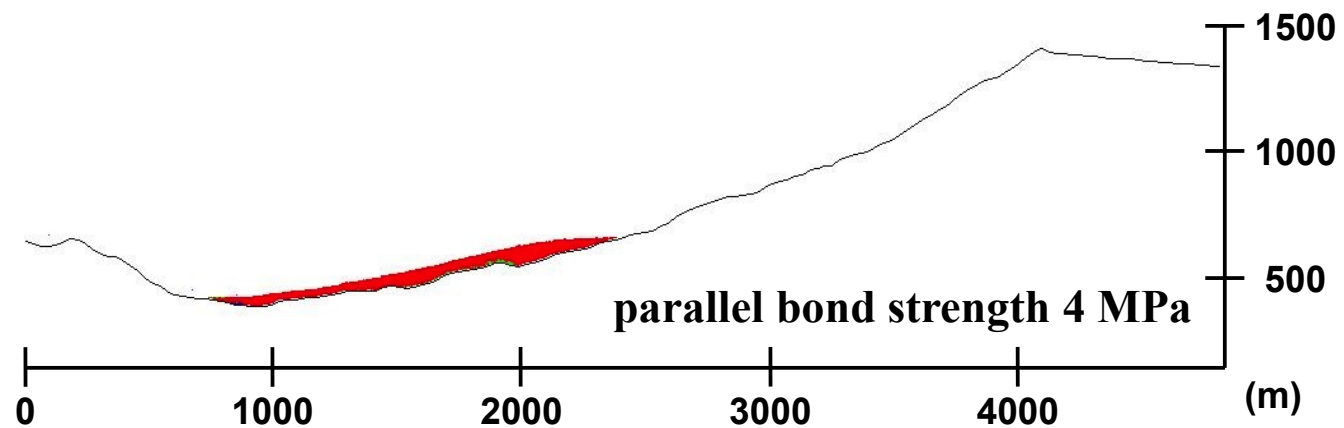
- Influence of particle size
- Influence of wall friction
- Influence of ball friction
- Influence of bonding between the particles
- ...

牆摩擦係數對崩塌距離之影響



球摩擦係數對崩塌距離之影響





A progressive failure of rockslide video

- Zheng-yi Feng 102年6月成大演講/MOV02D.MOD 或
[http://www.rts.ch/video/info/journal-continu/4913479-
effondrement-d-une-falaise-a-riddes-vs.html](http://www.rts.ch/video/info/journal-continu/4913479-effondrement-d-une-falaise-a-riddes-vs.html)
- Frequency vs size of landslide mass
- Notice the **low** frequency of the sound around **58 sec.**

Particle size: $1 \sim 2$ m

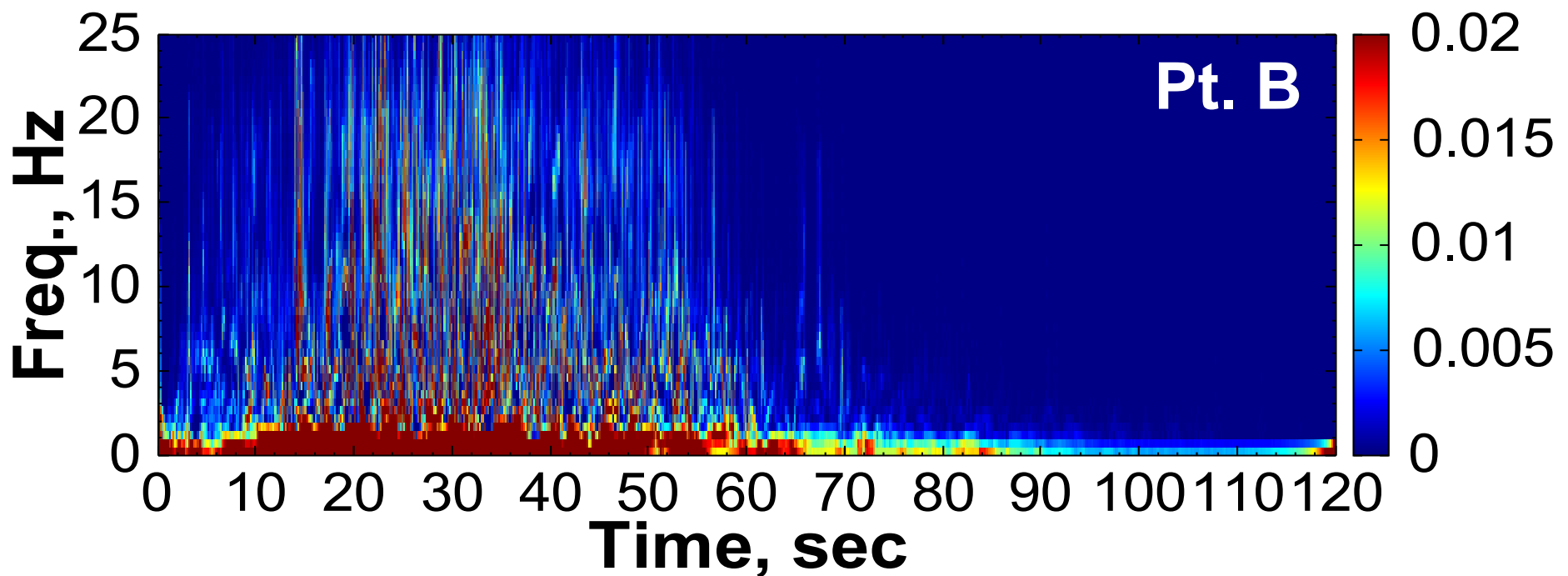


圖34 垂直速度之時頻圖(顆粒半徑 $1\sim 2$ m)

Particle size: 3~4 m

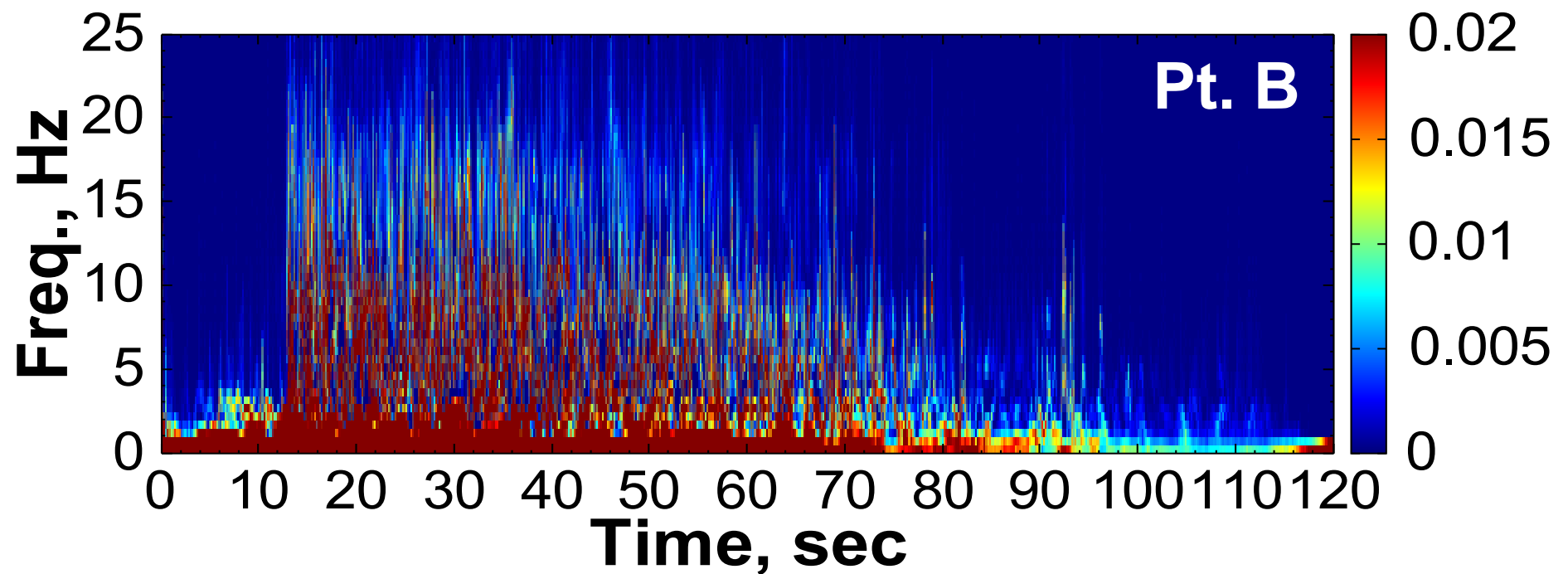


圖33 垂直速度之時頻圖(顆粒半徑3~4 m)

崩塌震動訊號特性分析結論

- 由比較時頻圖，顆粒越大，其震動訊號之頻率較為低頻。
- **鍵結強度**是影響崩塌流動距離與堆積型態的控制因素之一

大尺度邊坡模型沖蝕崩塌試驗初步成果

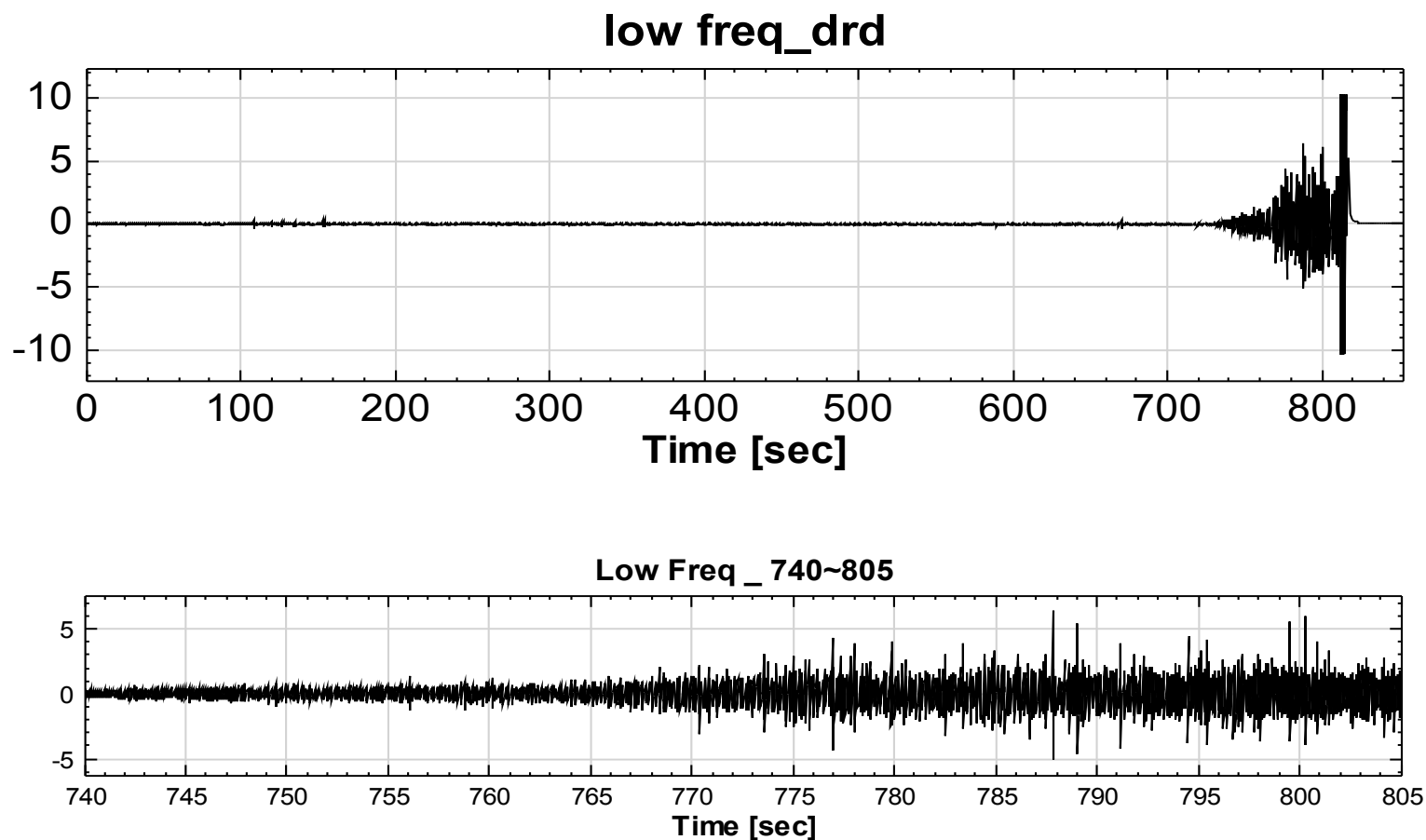
- An erosion test of an artificial slope
- Partial & Preliminary results of the test on 2013/10/14 and 2013/11/05 in Huisun



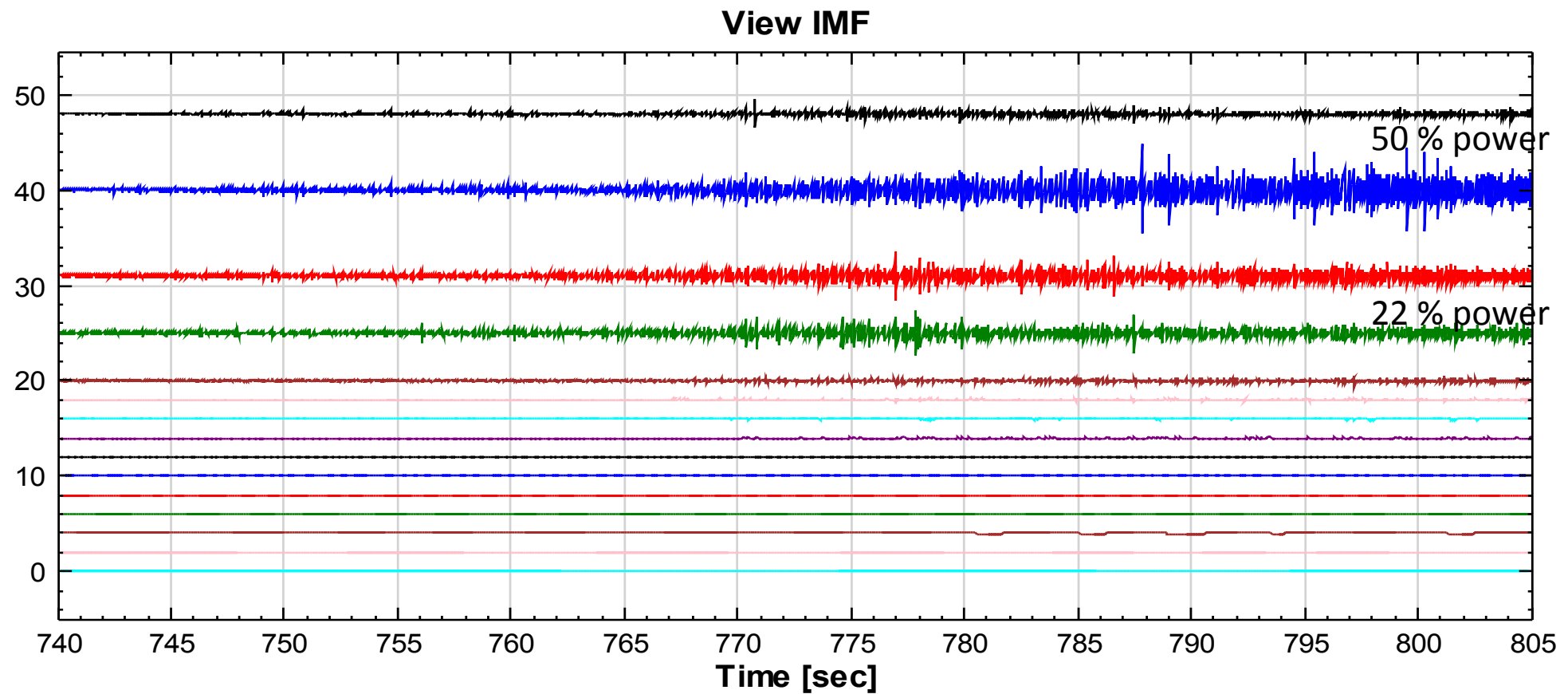


- The clip of the test #1 2013/10/14
- The clip of the test #2 2013/10/14
- The clip of the test #3 2013/11/05

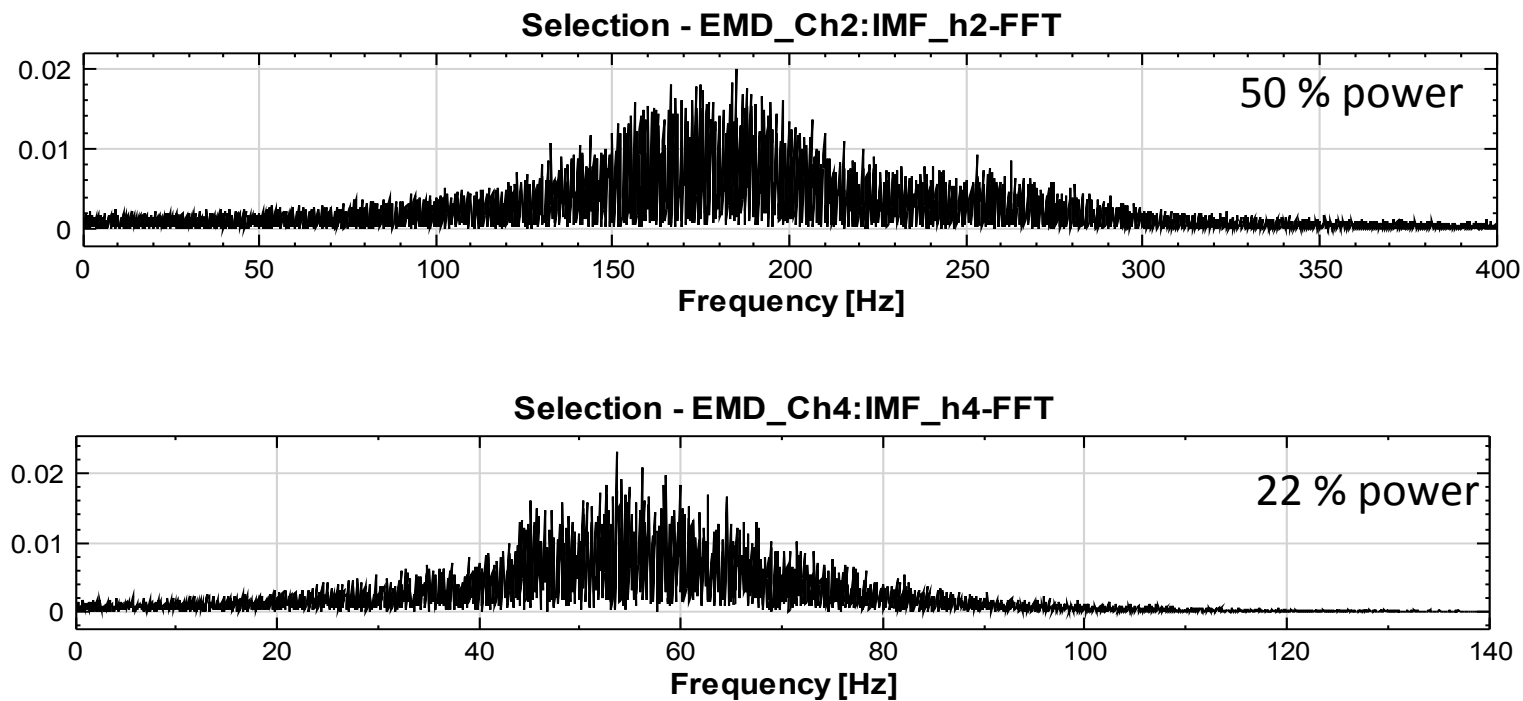
The original signal of the low freq sensor



The IMF of the low freq sensor



FFT of IMF 2 & 4 of the low freq. sensor



command

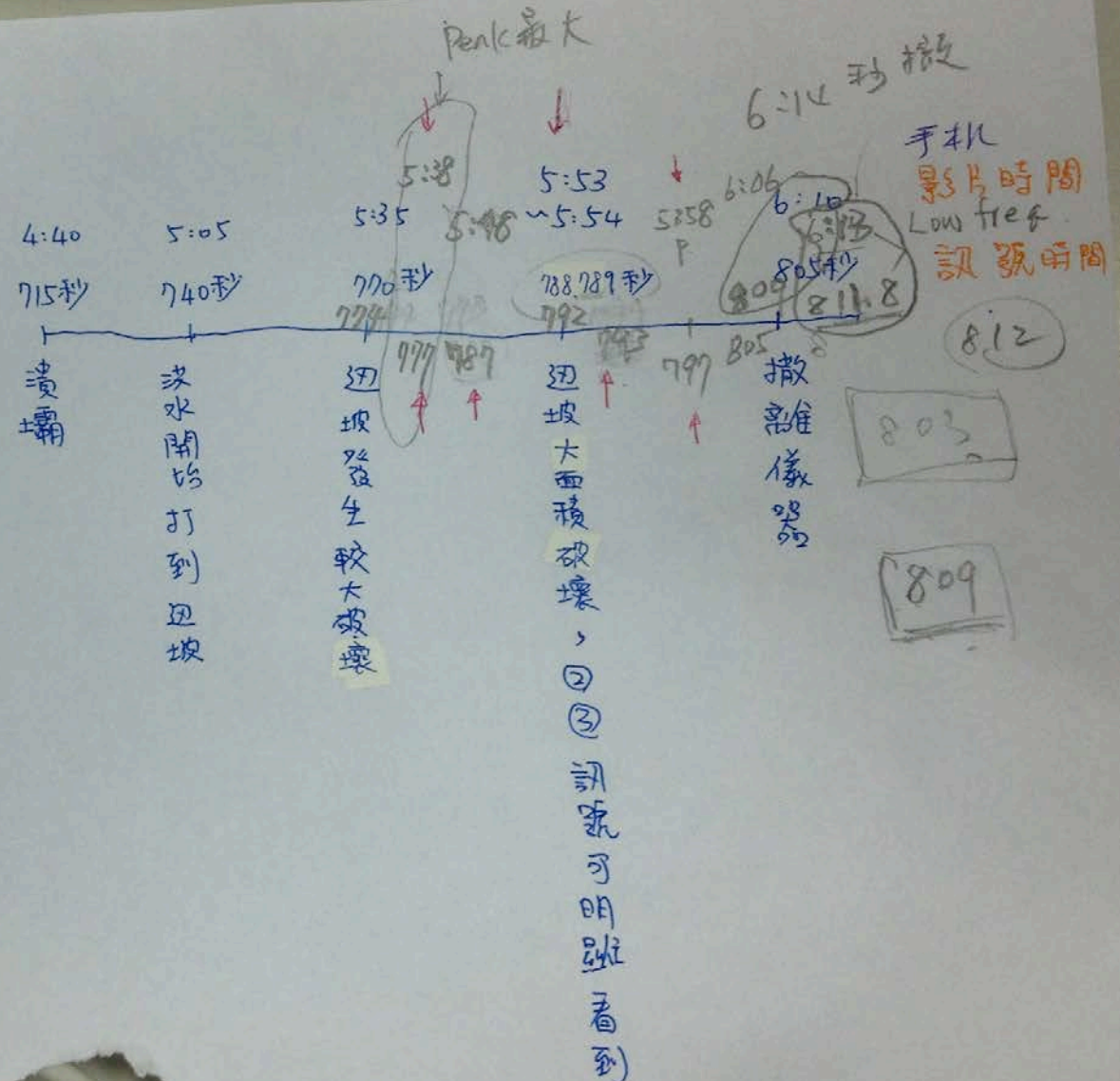
command

option

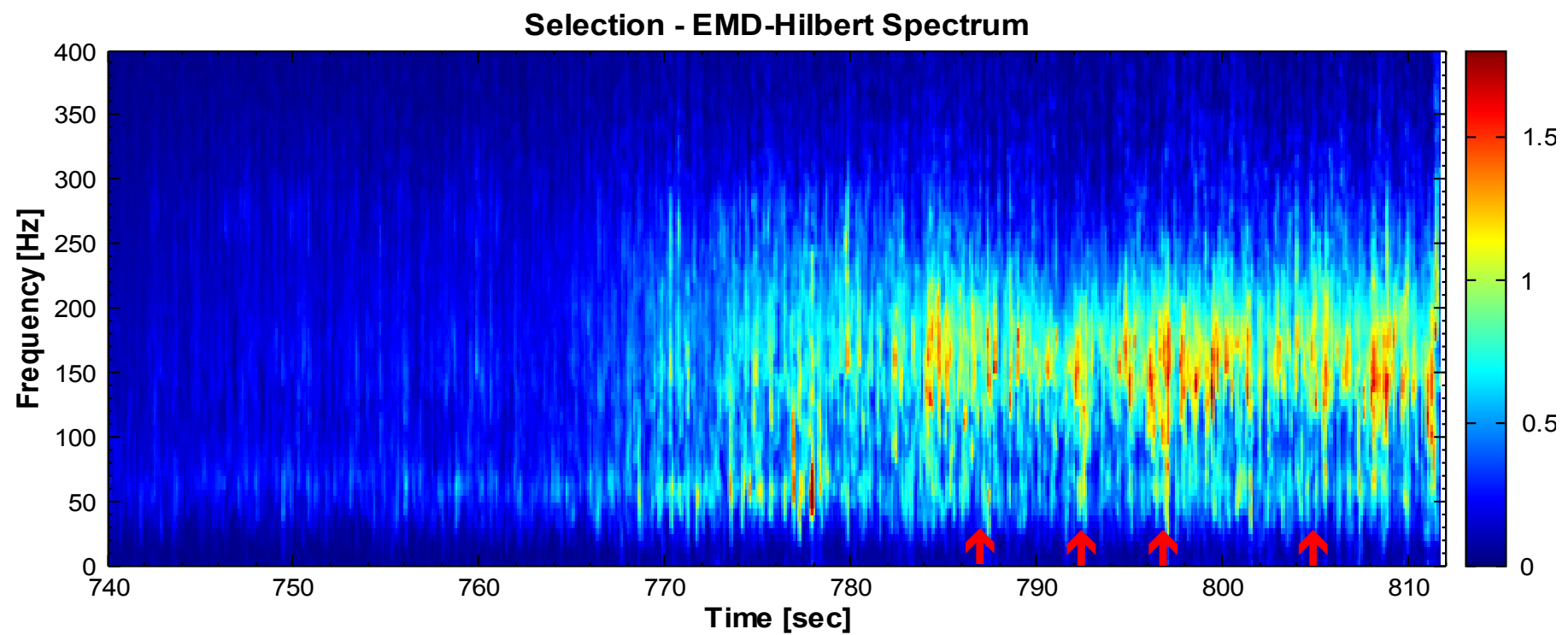
control

兩類
設
一起

- ① 坡上加速度規
- ② 坡下加速度規
- ③ 低頻加速度規
- ④ 水管內 microphone
- ⑤ 坡上方 microphone
(in air)

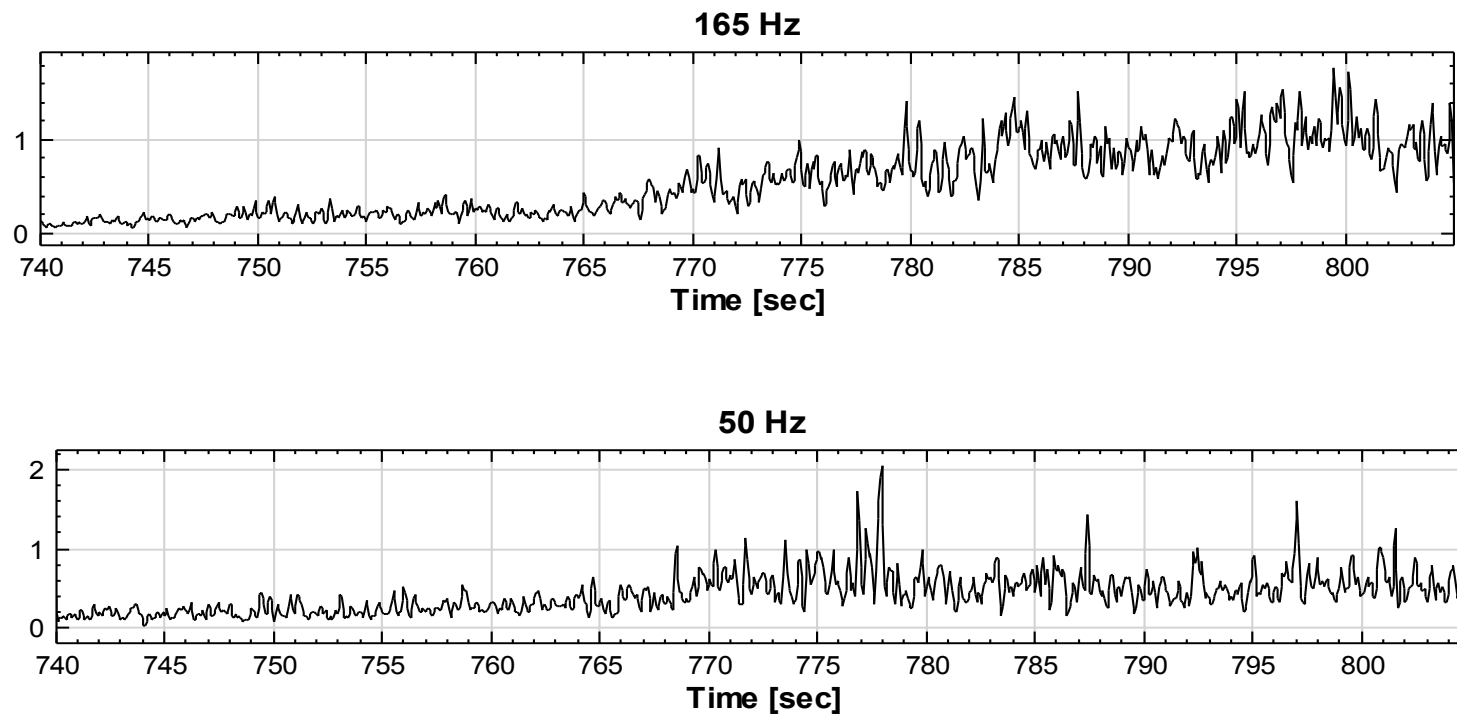


Time-freq spectra of the low freq. sensor

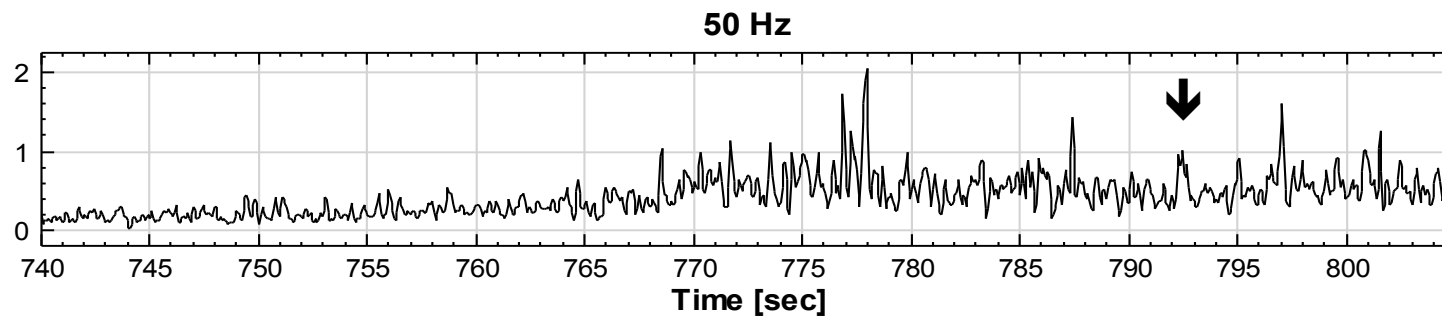


↑：表示有「明顯」崩塌時間點

Spectra magnitude of 50 & 165 Hz

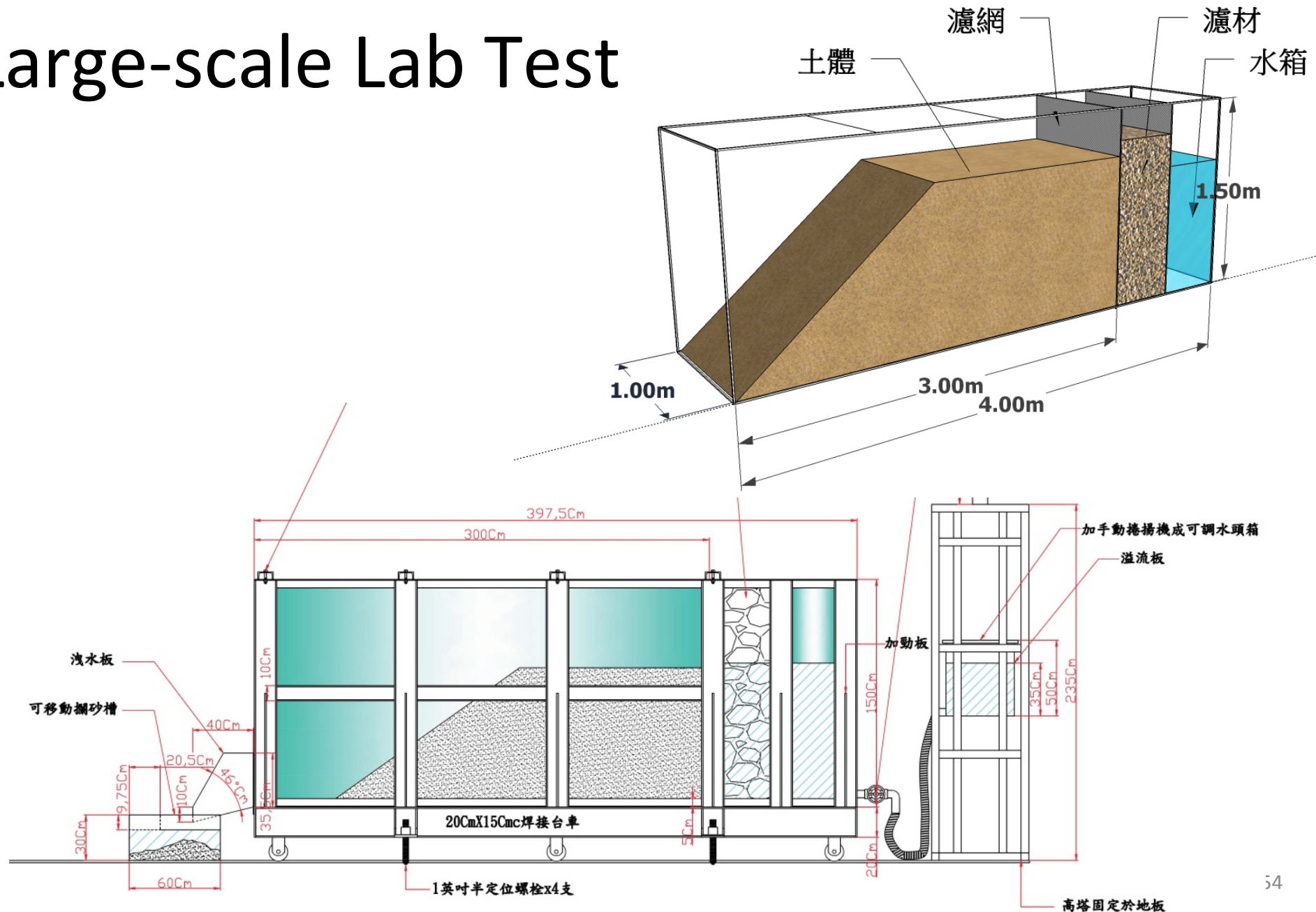


Spectra magnitude of 50 & 165 Hz



未來研究構思

Large-scale Lab Test



Large-scale Lab Test

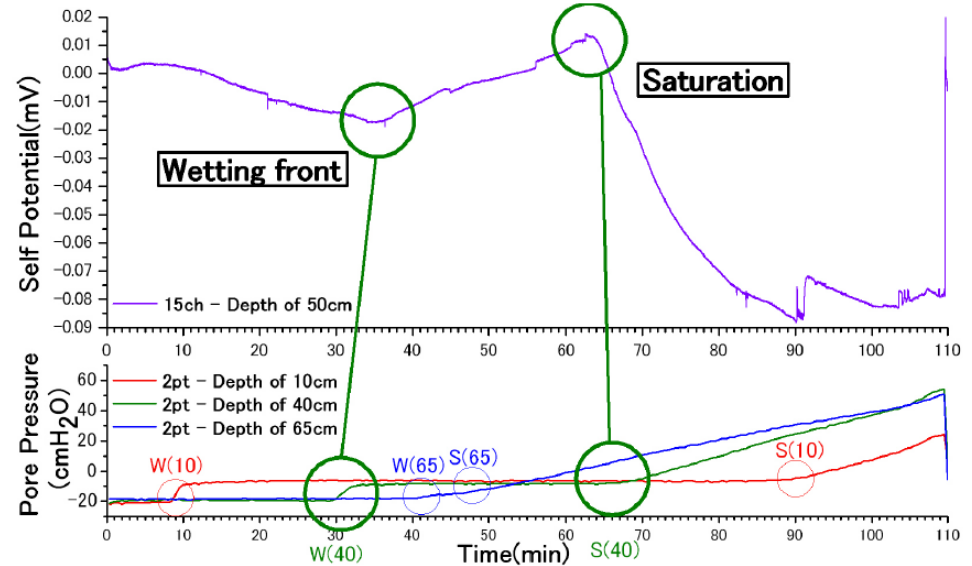


Sensors

- a. 非極化電極
- b. 土壤含水量感應器
- c. 基質吸力感測器
- d. 孔隙水壓計(Piezometer)
- e. 加速度感測器

電場(自然電位)

- 非極化電極



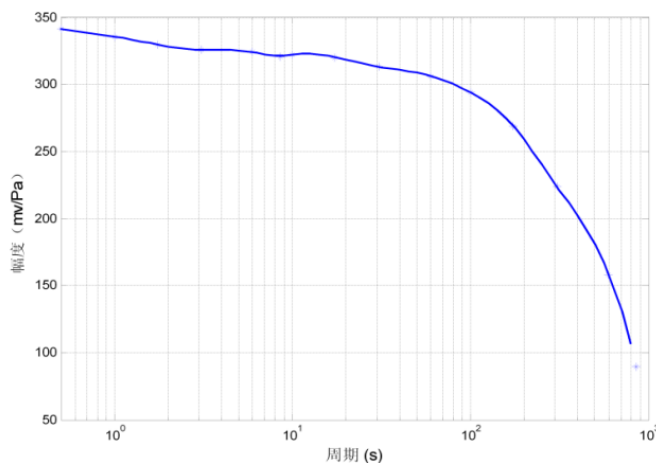
孔隙水壓 vs 自然電位變化(Hattori, et al. 2009)

- 感謝中大陳建志教授指導與協助!
- The clip of 室內大尺寸模型試驗 (縮時影片)

Infrasonic次聲 - 聽不到的聲音



(a) InSAS2008 Infrasound Sensor



(b) Frequency Sensitivity Curve of InSAS2008(No.0082)

- 中国科学院声学研究所研制

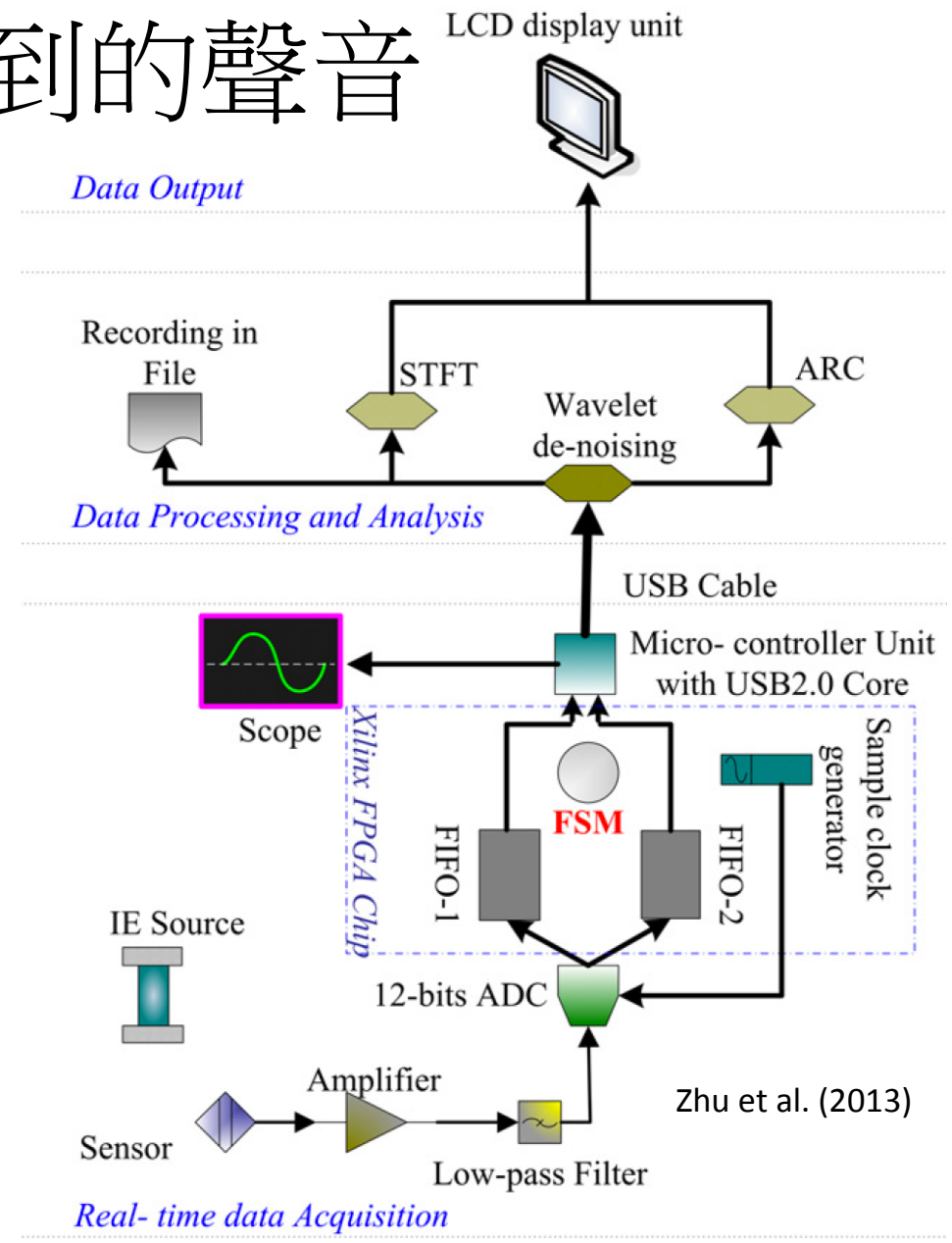
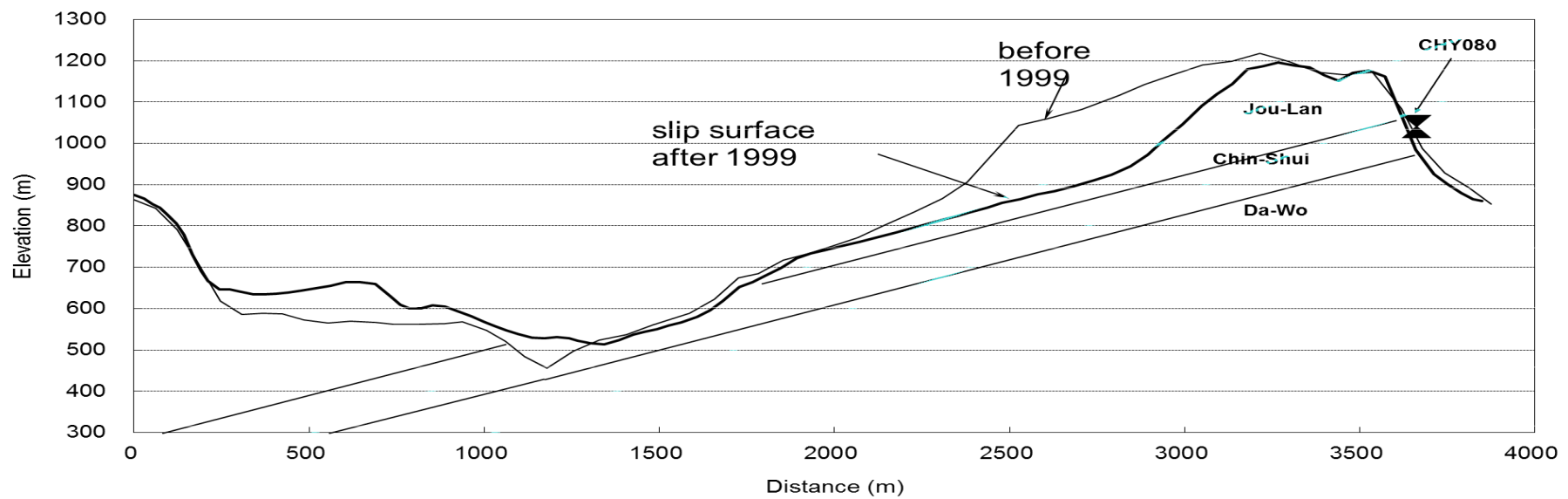


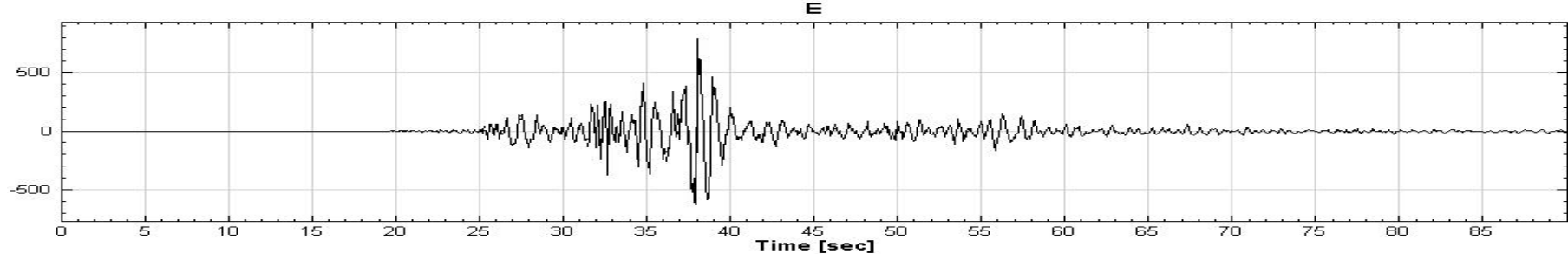
Fig. 3. Illustration of the infrasonic detector structure and work process.

震動訊號與地震訊號分離

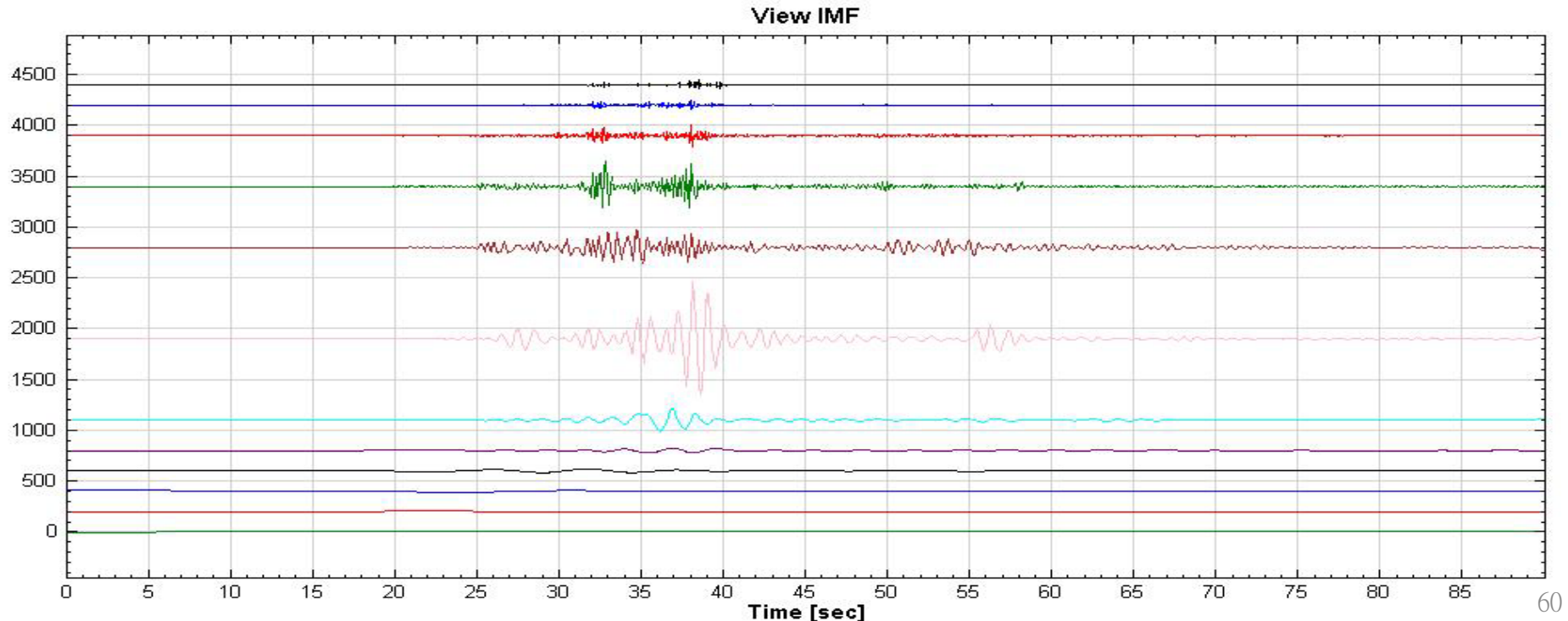
- 1999年921地震造成草嶺順向坡崩塌...



草嶺站CHY080 921震動訊號處理



- 假設25s至45s震動為地震引發，50s至65s為山崩。求證中！
- IMF5為主要能量來源。



未來研究著力點

- 電場(自然電位)
- Seismic & Infrasonic 次聲
- Pankow, et al. (2014) 提及：
 - Geometry of rock avalanche **vs** geophysical data
 - **seismic** and **infrasound signals** **vs** physical properties of the mass flows
 - long-period seismic radiation **vs** a single force modeling or more complex source modeling
- 山崩即時偵測、定位 (in real time)

- 本研究承蒙行政院**國科會**99-2625-M-005-004-MY3、102-2625-M-005 -009 計畫之經費補助方能進行，僅致謝忱。
- 感謝中央大學陳建志教授**電場**指導與協助!
- 感謝建國科大羅佳明助理教授**PFC模擬**指導。

Thank you very much
for your attention.

Zheng-yi Feng, Ph.D., P.E.

Department of Soil and Water Conservation
National Chung Hsing University
tonyfeng@nchu.edu.tw

